DOCKETED	
Docket Number:	20-MISC-01
Project Title:	2020 Miscellaneous Proceedings.
TN #:	238617
Document Title:	Nathan S Lewis Comments - Studies of Long Term Energy Storage in CA and the contiguous US
Description:	N/A
Filer:	System
Organization:	Nathan S Lewis
Submitter Role:	Public
Submission Date:	7/1/2021 9:14:40 AM
Docketed Date:	7/1/2021

Comment Received From: Nathan S Lewis
Submitted On: 7/1/2021
Docket Number: 20-MISC-01

Studies of Long Term Energy Storage in CA and the contiguous US

Attached are two studies of long-duration storage benefits and needs, and cost-effectiveness, in a reliable, 100% variable renewable electricity system. The differentiating feature of the work is that it is fully data-driven and based on 39 years of hourly weather data to extract the variability of the wind and solar resource over the lifetime of assets on an electricity grid. The first study was for the U.S. and the second one is for CA in light of SB100.

Additional submitted attachment is included below.

Environmental Science & Technology

pubs.acs.org/est

Article

Wind and Solar Resource Droughts in California Highlight the Benefits of Long-Term Storage and Integration with the Western Interconnect

Katherine Z. Rinaldi, Jacqueline A. Dowling, Tyler H. Ruggles, Ken Caldeira, and Nathan S. Lewis*

Cite This: https://doi.org/10.1021/acs.est.0c07848

Read Online

ACCESS | Metrics & More | Article Recommendations | Supporting Information

ABSTRACT: As reliance on wind and solar power for electricity generation increases, so does the importance of understanding how variability in these resources affects the feasible, cost-effective ways of supplying energy services. We use hourly weather data over multiple decades and historical electricity demand data to analyze the gaps between wind and solar supply and electricity demand for California (CA) and the Western Interconnect (WECC). We quantify the occurrence of resource droughts when the daily power from each resource was less than half of the 39-year daily mean for that day of the year. Averaged over 39 years, CA experienced 6.6 days of solar and 48 days of wind drought per year, compared to 0.41 and 19 for WECC. Using a macro-scale electricity model, we evaluate the potential for both long-term storage and more geographically diverse generation resources to minimize system costs. For wind-solar-battery electricity systems, meeting California demand with WECC generation resources reduces the cost by 9% compared to constraining resources entirely to California. Adding long-duration storage lowers system costs by 21% when treating California as an island. This data-driven analysis quantifies rare weather-related events and provides an understanding that can be used to inform stakeholders in future electricity systems.

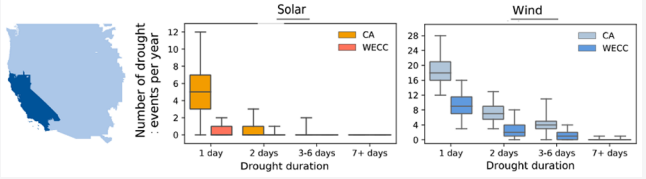

KEYWORDS: *California electricity system, variable renewable energy, zero-carbon electricity, macro-energy model, wind energy, solar energy, interannual variability*

Downloaded via STANFORD UNIV on April 6, 2021 at 19:32:52 (UTC).
See https://pubs.acs.org/sharingguidelines for options on how to legitimately share published articles.

INTRODUCTION

Numerous recently enacted U.S. state laws or regulations stipulate extensive utilization of wind and solar renewable energies before midcentury to facilitate deep decarbonization of electricity systems.[1−12] The inherent variability of these energy resources due to geophysical processes may require extensive curtailment of variable renewable generation if least-cost systems are to comply with resource adequacy planning standards. Analysis of the geophysical variability of wind and solar energy resources over multidecadal time scales for the contiguous United States (CONUS) indicates substantial mismatches between resource supply and electricity demand.[13] The duration and frequency of these gaps increases with decreases in the geographical area over which energy resources are aggregated.[13] Moreover, data over multiple decades is required to rigorously assess resource adequacy for electricity generation based primarily on variable renewable resources.[14−18] Collins et al. used 30 years of hourly wind and solar data to evaluate a European power system and concluded that studies based on a single or few years of data could not sufficiently capture the impacts of variability on variable renewable electricity (VRE) systems.[19] Using 30-years of daily data Raynaud et al. showed that wind, solar, and run-of-the river hydroelectric generation technologies all exhibit different drought behavior over this time-scale.[15] Recent use of reanalysis data sets to evaluate wind power in Germany,[16] Great Britain,[17] and regions across Europe[18] shows the necessity of using multidecadal data to capture the occurrences of rare but important extreme wind events. Clearly, understanding weather-related resource variability over multidecadal time scales is necessary to ensure reliability in wind- and solar-based electricity systems.

Within the United States, California is a leader in the development of such renewable electricity systems. California Senate Bill 100 (SB100) mandates[20] that 100% of retail in-state electricity sales must derive from eligible renewable or zero carbon resources by 2045. By 2030, 60% of electricity must come from specified renewable electricity sources, limiting the maximum firm generator dispatch, such as large hydropower or natural gas with carbon capture and sequestration (CCS), for future electricity systems. In 2018, the California Energy Commission estimated that 34% of California's retail electricity sales were provided by eligible renewable resources including wind, solar, biomass, geo-

Received: November 19, 2020
Revised: March 19, 2021
Accepted: March 19, 2021

ACS Publications © XXXX American Chemical Society

thermal, and small hydroelectric power.[21] Of these resources, wind and solar generation accounted for the largest portion of renewable electricity, providing about 70% of total renewable electricity generation.[21] California and the Western Interconnect (WECC) therefore provide important regional examples to analyze the relative impacts of imposing geographic restrictions on wind and solar electricity generation for a reliable decarbonized electricity system.

Long-term energy storage, supplemental generation, demand management, and transmission expansion are all potential options to provide reliability in 100% renewable electricity systems.[13,22−25] Low-carbon, firm generation technologies such as large-scale hydroelectricity, nuclear power, geothermal, biofuels, and natural gas with CCS could reduce both the costs of variable renewable electricity systems and the relative benefits of transmission expansion across larger geographic areas. However, such technologies are limited by legislation, constrained geographically and/or face major barriers to scale up.[6,22,23,26,27] It remains to be seen to what extent wind and solar generation in California and WECC will face similar barriers. We have framed this study based on an idealized electricity system that relies solely on wind and solar generation, thereby identifying an upper-bound for the influence of weather variability on system cost. Future work could include hydropower, which is influenced by altogether different weather variability on both seasonal and interannual time scales.

In systems dominated by wind and solar generation, accurate estimates of wind and solar generation capacities that ensure resource adequacy require decades of weather data.[13,19] In these systems, power systems operators will need to compensate for variations in these resources over both seasonal and interannual time scales and plan for extreme events wherein power generation from wind and/or solar is far lower than expected. Some studies have considered the variability of wind and solar resources over longer time-scales by analyzing fluctuations in wind speeds and solar irradiance.[28−31] Other studies use decades of historical weather data from reanalysis data sets to calculate the power output from wind and solar generators and consequently assess their variability.[13,32,33] The effects of this inherent resource variability on the interannual variability of metrics like generation costs and CO_2 output in power systems that rely heavily on wind and solar generation has also been examined.[19] Although more studies are focusing on the variability of wind and solar generation resources over long time-scales, little quantitative analysis exists regarding the frequency and duration of low-power events when the wind and/or solar generation potential falls well below the expected value. Matsuo et al. used 28 years of hourly meteorological data and showed that the balance between energy supply and electricity demand during these low-power events determined the required installed energy storage capacities for a zero-emission power system in Japan.[34] For the wind resource, Ohlendorf et al. quantified the occurrence of low power events in Germany using 40 years of reanalysis data and found that short low wind-power events of about five consecutive days occur yearly, whereas longer events lasting nearly eight consecutive days occur only every ten years.[16] For Great Britain, Cannon et al. evaluated extreme wind power events over 33 years and determined that these high and low power wind events can be approximated using a Poisson-like random process.[17] Weber et al. evaluated the statistics of these extreme wind power events in Europe and found that their distributions have heavy tails due to the multiple weather types and circulation patterns that cause the events to occur.[18] Raynaud et al. expanded this type of analysis to include wind, solar, and run-of-the-river hydroelectric generation for 12 regions in Europe and found that the characteristics of these drought events differ greatly between generation sources. Specifically, the wind resource is characterized by short and frequent power droughts; hydroelectricity generation is characterized by rare and long drought events; and solar drought events differ greatly depending on the region examined.[15]

For regions in the United States, various studies have analyzed the interannual variability of wind speeds,[30,31] solar irradiation,[28] and power generation of wind and/or solar resources.[13,32,33] Li et al. used 30 years of reanalysis data to evaluate wind speeds in the Great Lakes region of the United States and observed that, for this region, interannual variability is seasonally dependent, with winter months exhibiting more variability than summer.[30] Brower et al. showed the interannual variability of wind speeds based on 25 years of global reanalysis data for a variety of regions including the United States. They observed that the interannual variability of the wind resource varies greatly depending on the region examined and that, for the western United States, the interannual variation of mean wind speeds is generally around 5−6%.[31] For the solar resource, Gueymard et al. used data from the National Solar Radiation Database from 1998 to 2005 to evaluate the spatial and temporal variability of solar irradiation across the United States.[28] Studies that explore the fluctuations in power generation due to the inherent variability of the wind and solar resources generally show variations over long time-scales that decrease when resources are aggregated over larger areas. Over the entire contiguous United States, Shaner et al. used 36 years of hourly weather data to quantify the covariability of wind and solar resources.[13] At smaller regional scales, Rose et al. used 32 years of reanalysis data to examine wind power at sites across the Great Plains region in the United States.[33] Kumler et al. used Texas as a regional example to demonstrate the interannual variability of both wind and solar electricity generation.[32] However, none of these studies evaluate both wind and solar generation in California. Furthermore, within the United States, quantification of the occurrence of resource droughts is limited. Handschy et al. evaluated nine sites across the United States using simulated wind power and demonstrated that the probability of having a low-power wind event shrinks exponentially with the number of aggregated sites.[35] In contrast, we identify herein the frequency and duration of resource droughts for wind and solar generators in both California and the Western Interconnect using 39 years of historical weather data. Through quantifying these resource drought events over the period from 1980 to 2018, we directly identify rare but extreme weather-related events and provide an understanding that can be used to inform asset deployment in a region with ambitious climate legislation requiring 100% of electricity generation from zero carbon resources by 2045.[6]

With a quantitative understanding of the variability and availability of wind and solar generation over a multidecadal time scale, we then explore pathways to address this issue in a 100% reliable wind- and solar-based electricity system. Many analyses that explore potential end-states or transition pathways to wind- and solar-based electricity systems utilize specified or constrained capacities and dispatch schedules, idealized demand curves, and/or theoretical or few years of

https://doi.org/10.1021/acs.est.0c07848
Environ. Sci. Technol. XXXX, XXX, XXX−XXX

Table 1. Cost and Technological Assumptions[e]

	Wind	Solar	PGP[d] storage	To PGP[d]	From PGP[d]	Battery storage	To and from battery
Assumptions from U.S. Energy Information Administration[42] except when otherwise noted							
Technology description	Wind turbines, onshore	Solar PV, single-axis tracking	Underground salt cavern[a]	PEM electrolysis, plus compression[a]	Molten carbonate fuel cell, CHP	Li-ion battery	Li-ion battery
Technology type	Generation	Generation	Storage (of H_2)	Conversion (produce H_2)	Conversion (consume H_2)	Storage	Conversion
Capacity (fixed) cost type	Power capacity ($/kW)	Power capacity ($/kW)	Energy capacity ($/kWh)	Power capacity ($/kW)	Power capacity ($/kW)	Energy capacity ($/kWh)	Power capacity ($/kW)
Capacity (fixed) cost	1657	2105	0.16[b],[43]	1058[44]	5854[45]	261[46]	1568[46]
Project life (yrs)	30	30	30[47]	12.5[44,47]	20[45]	10[48]	
Discount Rate	0.07	0.07	0.07	0.07	0.07	0.07	
Capital recovery factor(%/yr)	8.06	8.06	8.06	12.26	9.44	14.24	
Fixed O&M cost ($/yr)	47.47	22.02	0	0	0	0	
Round-trip efficiency			49%[c],[44,45]			90%[49]	
Self-discharge rate			0.01% per year[50]			1% per month	(6 h charging time)
Annualized capital costs paid hourly							
Fixed cost	0.021 $/kW/h	0.022 $/kW/h	$1.47 \times 10^{-6}$$/kWh/h	0.0148 $/kW/h	0.063 $/kW/h	0.004 $/kWh/h	
Variable cost	0.000 $/kW/h	0.000 $/kW/h	0.000 $/kWh/h	0.000 $/kW/h	0.000 $/kW/h	0.000 $/kWh/h	

[a]For more detail on underground H_2 storage costs, and fixed costs and lifetimes of polymer electrolyte membrane (PEM) electrolyzers and compressors, see Dowling et al.[25] [b]This cost is equivalent to $6.3/kg H_2. The higher heating value (HHV) is 39.4 kWh/kg H_2. [c]PEM electrolyzers and molten carbonate fuel cells with combined heat and power (CHP) are both modeled as 70% efficient. [d]Here, PGP refers to Power-to-Gas-to-Power, comprising a long-term energy storage technology. [e]Costs and technological assumptions for wind, solar, power-to-gas-to-power, and batteries used for the base case simulation. See model formulation in Section S1 for more detail.

historical wind and solar resource data. Williams et al. investigated the infrastructure and technology pathways to achieve deep greenhouse gas emissions cuts in California by 2050 and demonstrated the importance of the electricity sector in achieving these goals.[36] Similarly, an intermodel comparison of nine energy models that examined greenhouse gas emissions for California demonstrated increases in total power generation as well as increases in the fraction of total generation provided by variable renewable generation for all deep greenhouse gas reduction scenarios.[37] The majority of the new generation infrastructure in these scenarios came from wind and solar generation.[37] Using one year of weather data, Colbertado et al. demonstrated the importance of hydrogen storage in achieving 100% renewable electricity for the state of California.[38] Ziegler et al. used 20 years of wind and solar data to determine target energy storage costs to meet various output profiles for Arizona, Iowa, Massachusetts, and Texas.[24]

The current North American Electric Reliability Corporation (NERC) resource adequacy planning criterion stipulates that there shall be no more than 1 h in a decade when hourly averaged demand is not met due to constraints associated with resource availability, i.e., >99.998% of hourly demand must be met over multidecadal time periods.[13,39] Here, we use hourly weather data in conjunction with historical electricity demand data retrieved from the U.S. Energy Information Administration (EIA) demand database and cleaned to replace extreme outlier values with plausible imputed values.[40] The first section of the analysis examines the variability and availability of wind and solar resources using these data. We quantify the occurrence of resource droughts when the daily power derived from both wind and solar resources was less than half of the 39-year daily mean for that day of the year for each resource. We then specify electricity systems with different wind/solar mixes where the electricity generation over the period from 1980 to 2018 is equal to that of the electricity demand. Using these specified capacities of wind and solar and the hourly capacity factors derived from the MERRA-2 reanalysis weather dataset we then determined the frequency and duration of the gaps between wind and solar supply and electricity demand for California and WECC. Due to limited historical data availability, the demand profiles do not always correspond to the same meteorological weather year as modeled solar and wind generation (see Methods for more details).

In the second section of the analysis, we used a macro-scale electricity model[41] to evaluate the potential for both long-term storage (here, power-to-gas-to-power) and expansion of resource aggregation area to minimize overall system costs for 100% reliable systems powered by 100% variable renewable electricity generation. Estimated current asset costs (Table 1) were used throughout to compare on a consistent basis the relative impacts of geographic constraints and geophysical resource variability on system costs. The least-cost solutions represent idealized systems with installed capacities and dispatch schedules that assume perfect foresight of both weather and electricity demand. We assumed lossless transmission across the various regions of interest to readily extract the key dynamical relationships between the various parameters of interest. Low-dimensional models with few state variables are unlikely to accurately project how a real system would evolve dynamically as it is deployed amidst uncertain costs subject to changing policy, electricity demand, and market forces. Our examination of idealized cases is intended to guide those working with more detailed and comprehensive models toward interesting areas of parameter space to explore.

https://doi.org/10.1021/acs.est.0c07848
Environ. Sci. Technol. XXXX, XXX, XXX−XXX

METHODS

Resource, Data, and Code Availability. Direct all requests for further information, resources, and materials to Katherine Z. Rinaldi, kat@caltech.edu. In the interest of transparency, the model code, input data, and analytical results from the macro energy model (MEM) are publicly available on GitHub at https://github.com/carnegie/SEM_public/tree/Rinaldi_et_al_2021.

Calculating Wind and Solar Capacity Factors. This study utilizes hourly wind and solar capacity factors estimated using the Modern-Era Retrospective analysis for Research and Application, Version-2 (MERRA-2) reanalysis satellite weather data (horizontal resolution = 0.5° by latitude and 0.625° by longitude).[51]

To calculate solar capacity factors, we determine the solar zenith angle and incidence angle based on the location and local hour[52,53] and then estimate the in-panel radiation.[54] We use an empirical piecewise model that takes into account both ratios of surface to top-of-atmosphere solar radiation (the clearness index) and the local time to separate the direct and diffuse solar components.[55] We assume a horizontal single-axis tracking system, with a tilt of 0° and a maximum tuning angle of 45°. The use of a tracking system minimizes variability, as compared to flat plate solar panels, and moreover improves solar availability. Our use of single-axis trackers primarily excludes rooftop solar installations from this study but produces less variability and increased potential for solar electricity generation. We use a performance model, which considers both the surrounding temperature and the effect of irradiance, to calculate the power output from a given panel.[56,57]

To calculate wind capacity factors, we interpolate the raw wind speed data to 100 m (to match the assumed 100 m hub heights) by assuming a power law, based on wind speed at 10 and 50 m. We employ a piecewise function which consists of four parts: (1) for a cut-in speed (u_{ci}) less than 3 m s^{-1} the capacity factor is zero, (2) between a cut-in speed of 3 m s^{-1} and rated speed (u_r) of 12 m s^{-1} the capacity factor is u_{ci}^3/u_r^3, (3) between a rated speed of 12 m s^{-1} and cut-out speed (u_{co}) of 25 m s^{-1} the capacity factor is set to 1, and (4) above a cut-out speed of 25 m s^{-1} the capacity factor is zero.[13,58]

The solar and wind capacity factors are estimated with the same resolution as MERRA-2 for each grid cell in CONUS, WECC including CA, WECC excluding CA, and CA. See Figure S14 for more information on the shapefiles used to define these geographical regions. We then selected grid cells over land where the annual mean capacity factor is larger than a threshold value of 26% for both solar and wind. The resulting average capacity factors over the 39-year period were similar to those reported for utility scale generation of wind and solar in the U.S.[59] This threshold includes 90 and 5 of the total possible grid cells for solar and wind, respectively for CA, 557 and 380 for WECC, and 467 and 375 for the portion of WECC excluding CA.

EIA Demand Imputation. In July 2015, the EIA began collecting hourly electricity demand information across CONUS via the EIA-930, where values are calculated by each reporting balancing authority (BA) individually.[60,61] An application programming interface was used to query the original EIA data from their open data database on September 10, 2019. These data offer the most temporal granularity in publicly available demand data for the contiguous U.S. but nevertheless contain substantial quantities of missing and outlier values. These missing and outlier values were replaced with plausible values by developing a data cleaning method that flagged the most extreme outliers and then used a multiple imputation by chained equations (MICE) technique to impute the missing values.[40] The cleaned data are publicly available.[62] For all scenarios in this paper, we use data from a single demand year (2018) looped over the 39-year period, such that interannual variations are solely due to weather-related events, as opposed to changes in electricity demand from year to year. For leap years, we repeat the demand data from February 28 for February 29.

Resource Adequacy Analysis. We calculate the percent of demand met for each day in the 39-year period from 1980 to 2018 as a function of resource mix (Figure 3, Figure S4). For each geographical region, we calculate the installed solar and wind capacities using the specified resource mix, the hourly resource data, and the generation value. For the resource mix, if X% of electricity generated is from solar, the remaining electricity generation ((100-X)%) is from wind. We build the electricity system such that the electricity produced by solar and wind over the 39-year period is equal to the total electricity demand over the same period. We then use the hourly resource data derived from MERRA-2 to determine the power generated for each hour. We loop a single year of demand data (2018) over the entire 39-year period such that the demand is consistent and we are only observing interannual variations due to weather-related events. We then calculate percent demand met by dividing the power generated from the built system by the electricity demand for each hour from 1980 to 2018. We assume no operational outages or system energy losses, so for our purposes, "reliability" represents any instance in which demand is not met solely due to a lack of dispatched supply from generation assets.

Cost and Technological Assumptions. The costs for all technologies including power- and energy-capacity costs for storage technologies (power-to-gas-to-power (PGP) and batteries) and discounted fixed costs are presented in Table 1. We assumed zero variable costs for all technologies. As noted in the table, wind and solar costs are taken from the U.S. EIA's 2018 Annual Energy Outlook.[42] Although these capital costs are lower in the more recent 2020 Annual Energy Outlook and other references,[63−65] we utilized the 2018 values so that our cost assumptions matched our previous analyses for CONUS, to facilitate comparison between results for different geographical regions.[25] This baseline year cost assumption should not substantially change the conclusions reached in this study regarding relative costs of various cases of interest, but may lead to slightly overestimated absolute system costs.

For PGP, we used the fixed costs, lifetimes, and efficiencies from the H2A model data compiled by the National Renewable Energy Laboratory (NREL).[43−45,47] For batteries, we estimated values from Lazard, a financial advisory and asset management firm, which bases the cost, energy capacity, and lifetime on usable energy capacity, as opposed to nameplate capacity.[48] Battery storage characteristics fall within the ranges provided by Lazard and were taken from Davis et al. and Pellow et al.[46,49] To account for the assumed 100% operational uptimes for storage technologies (batteries and PGP) employed here, results should be scaled proportionately in either the cost or the installed asset capacity to include a buffer against scheduled outages. For additional information on costs, see Section 3 of the Supporting Information.

https://doi.org/10.1021/acs.est.0c07848
Environ. Sci. Technol. XXXX, XXX, XXX−XXX

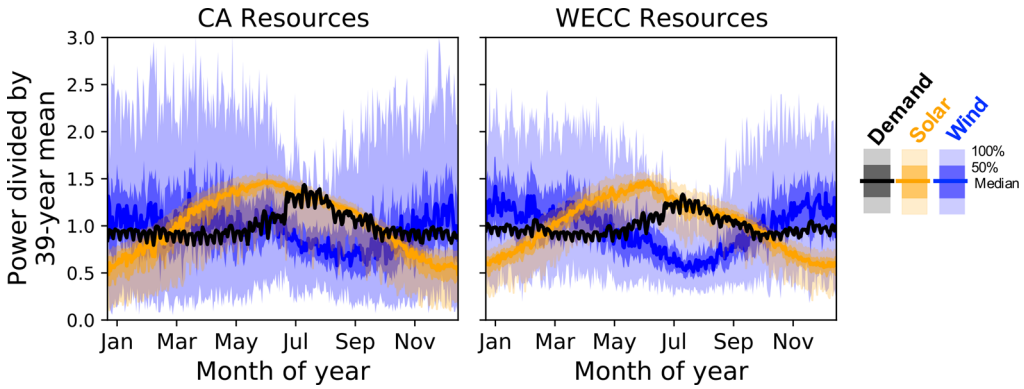

Figure 1. Temporal variability of wind (blue) and solar (yellow) resource supply over both California and the Western Interconnect during the 39-year period from 1980 to 2018. Seasonal variability of a single year (2018) of electricity demand (black). The dark line shows the median value while the darker and lighter shadings show the 25th to 75th and 0th to 100th percentiles of data, respectively. All data are normalized to their respective mean over the time period. This figure is adapted from Shaner et al.[1]

Macro Energy Model. The model used in this study utilizes a linear optimization to minimize system cost. We input cleaned hourly demand data from the EIA, wind and solar capacity factors derived from MERRA-2, and current representative EIA costs for solar, wind, and storage technologies (Table 1). The model then minimizes overall system cost and solves for installed capacity and hourly use of each technology while meeting 100% of electricity demand. For the scenarios explored in Figure 4, we use the 2018 values for wind and solar capacity factors and electricity demand data to optimize over the year. We also analyze simulations over 1-, 2-, 3-, 4-, 5-, and 6-year weather periods over the 39-year period while keeping the demand year constant (2018) to observe the effects of long-term planning on results (Figure S6, Figure S7, Table S8, Table S9, Table S10, Table S11). Analysis of longer time periods was computationally intractable. For more details on the objective function and model constraints, see the Supporting Information, Section 1.

RESULTS

Quantification of the Variability of Wind and Solar Resources in CONUS, WECC, and California. Figure 1 shows the hourly averaged variability of wind and solar resources over California as well as over WECC during the 39-year period from 1980 to 2019. For comparison, the variability of wind and solar resources aggregated across CONUS[13,25] is shown in Figure S1. Wind and solar resources demonstrate substantial interannual variation during the multidecadal time period. In California, the maximum difference in wind daily mean capacity factors occurred on the 93rd day of the year, in early April, with a minimum of 0.04 and a maximum of 0.93: a range of 0.89. For WECC, the maximum difference occurred on the 308th day of the year, in early November, where the daily mean capacity factor for wind on that day ranged from a minimum of 0.08 to a maximum of 0.85: a slightly smaller range of 0.77. In a previous analysis for CONUS,[25] the maximum difference in wind daily mean capacity factors occurred on the 333rd day of the year, in late November, with a minimum of 0.09 and a maximum of 0.80: a range of 0.71.[25] Clearly, increases in the area over which these renewable resources are aggregated decreases interannual variability, especially in the wind resource.

We defined a "resource drought" as a period of days for which the daily mean capacity factor for wind and/or solar was less than 50% of the mean capacity factor over the 39-year period for that day of the year (see Figure S2, Figure S3, Table S1, and Table S2 for results with different threshold cutoffs and capacity factor cutoffs). For example, in California, the average wind capacity factor for January 1st over the 39-year period was 0.34. The seven January 1sts for which the daily mean capacity factors were 0.17 or less were then considered resource drought days. Figure 2 indicates that both

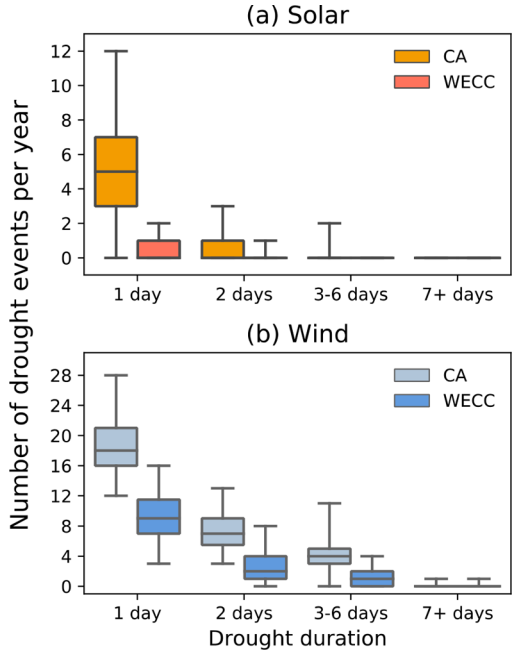

Figure 2. Resource droughts in CA and WECC. Box and whisker plots show the distribution of drought events per year for each year during the 39-year period from 1980 to 2018 for the (a) solar and (b) wind resources. Whiskers represent the minimum and maximum of each data set. Drought events are days where the mean daily capacity factor for solar or wind was less than 50% of the mean daily capacity factor for that day of the year over the 39-year period for a duration of 1-, 2-, 3−6, or 7+ days. Resource droughts greater than 1-day in duration are not also counted toward 1-day occurrences. Drought events are counted toward the year in which the drought begins. Orange and light blue bars represent CA solar and wind droughts, respectively, while red and dark blue bars represent WECC wind and solar droughts. This figure is supported by Table S4 and Table S5.

https://doi.org/10.1021/acs.est.0c07848
Environ. Sci. Technol. XXXX, XXX, XXX−XXX

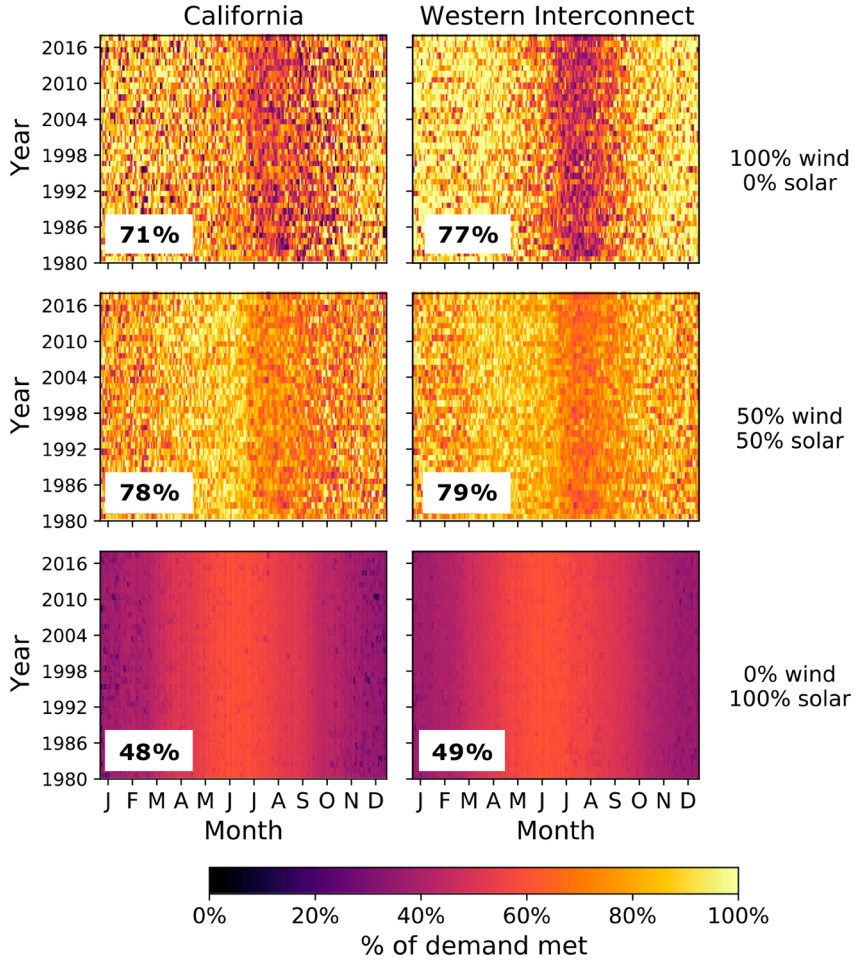

Figure 3. Percent demand met for each day over the 39-year period from 1980 to 2018 for wind and solar based electricity systems. Each plot shows the potential of renewable resources to meet electricity demand for California (left column) and the Western Interconnect (right column). Each row corresponds to a different wind/solar generation mix. Marked percentages refer to the reliability (% of demand met) over the entire 39-year period for each region and mix.

occurrences of resource droughts and the interannual variability of drought events increased when resource utilization was restricted to be only over California instead of over the entire WECC region. For single day events in California, the number of solar drought events ranged from a minimum of 0 to a maximum of 12 events per year. For the larger region of WECC, the number of single day solar drought events only ranged from a minimum of 0 to a maximum of 2 events per year. Over the entire 39-year period, CA experienced 256 days of solar drought (6.6 days/yr) compared to only 16 for WECC (0.41 days/yr) and 14 for CONUS (0.36 days/yr) (Table S3). Of these days, about 30% of CA solar drought days occurred within groupings of greater than 1 day, with the longest solar drought period lasting 6 days. For WECC, all of the solar drought instances lasted a single day except for one occurrence that lasted 2 days. For CONUS, only single-day solar drought events occurred. In the wind resource, the number of single day drought events in California ranged from a minimum of 12 to a maximum of 28 events per year. For WECC, the number of single day wind drought events ranged from a minimum of 3 to a maximum of 16 events per year. From 1980 to 2018, California experienced 1884 total days of wind drought (48 days/yr) compared to only 732 in WECC (19 days/yr) and 316 in CONUS (8.1 days/yr) (Table S3). Although all regions experienced days of consecutive wind drought, California experienced four wind resource droughts that lasted a week or more (with the longest at 10 days), while WECC only experienced 1 week-long wind drought and CONUS did not experience any.

To examine the interplay of the daily and seasonal cycles of wind and solar generation and electricity demand as well as the effects of the inherent variability of both the wind and solar resources, we evaluate a system for which the electricity generated over the 39-year period is equal to electricity demand over the same period. Figure 3 shows the percent of daily electricity demand met for California and the Western Interconnect for each day in the 39-year period assuming that the total installed generation (wind+solar) capacities in each case was sufficient to generate the total integrated electricity demand over the 39-year period. We varied from 0% to 100% the fraction of solar capacity relative to total generation capacity (for additional wind/solar mixes for CA, WECC, and CONUS see Figure S4), where a 50% solar fraction refers to a system in which solar resources generate 50% of total electricity. Each wind/solar mix met a higher percentage of electricity demand in CONUS than in WECC than in California, with overall percent demand met over the 39-year period for solar fractions (as a percentage of total wind and solar generation) of 100%, 50%, and 0%, respectively: 81%, 80%, and 50% for CONUS; 77%, 79%, and 49% for the

https://doi.org/10.1021/acs.est.0c07848
Environ. Sci. Technol. XXXX, XXX, XXX−XXX

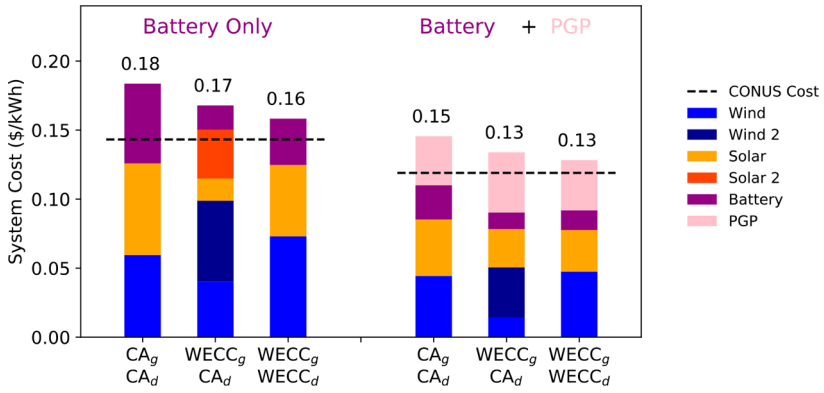

Figure 4. System costs for different resource and demand regions and technology combinations. For bars labeled CA_g CA_d, CA electricity demand is met with CA wind/solar generation. For bars labeled $WECC_g$ CA_d, CA electricity demand is met with wind/solar generation from both CA and the rest of WECC. For bars labeled $WECC_g$ $WECC_d$, WECC electricity demand is met with WECC wind/solar generation. The leftmost three bars represent systems with battery storage only whereas the rightmost three bars represent systems with both battery and PGP storage. Stacked areas in each bar correspond to the total system cost contribution from each technology over the optimization period (2018). The horizontal dashed lines refer to the system costs for wind-solar-battery electricity systems (left) and wind-solar-battery-PGP systems (right) for CONUS. For $WECC_g$ CA_d systems, Solar 2 and Wind 2 refer to the solar and wind resources from the rest of the Western Interconnect (excluding California). This plot is supported by Table S6 and Table S7.

Western Interconnect; and 71%, 78%, and 48% for California (Figure 3, Figure S4 for CONUS).

For both California and WECC, wind-heavier mixes yielded higher percentages of demand met (Figure S4). However, such wind-heavy mixes are likely not practically realizable if generation is constrained to occur exclusively in California, due to the limited geographical availability of the regional wind resource. Moreover, even with the optimal wind/solar generation mix, substantial overbuild would be necessary for either California, WECC, or CONUS to satisfy the North American Electric Reliability Corporation (NERC) requirement of >99.998% resource adequacy.[13,39] Dealing with these gaps caused by the geophysical variability in the wind and solar resources is thus essential to reliably meet electricity demand.

Grid Expansion and Addition of Storage Technologies Can Reduce System Costs. To explore potential end-states that fill these gaps in a cost-effective way, we employ a Macro Energy Model that uses wind and solar capacities and electricity demand from a single optimization year (2018) to solve for installed capacities and hourly use of generation and storage technologies. We used current technology costs to evaluate three different notional, idealized scenarios that included cases with or without long-term storage. We modeled 100% variable renewable, 100% reliable electricity systems for which California generation resources were used to meet California electricity demand (CA_g CA_d), generation resources from both California and the rest of the Western Interconnect were used to meet California electricity demand ($WECC_g$ CA_d), and generation resources from the Western Interconnect were used to meet the electricity demand of the Western Interconnect ($WECC_g$ $WECC_d$). Results for least-cost systems obtained by these optimizations are summarized in Figure 4 and Table S6.

For least-cost systems with or without long-term storage, the highest total system costs (in $/kWh delivered) were for CA_g CA_d, at 0.18 $/kWh for wind-solar-battery systems and 0.15$/kWh for wind-solar-battery-PGP systems (where PGP is power-to-gas-to-power, comprising a long-term energy storage technology). In all scenarios, the addition of long-term storage lowered system costs (from 0.18 to 0.15 $/kWh for CA_g CA_d, from 0.17 to 0.13 $/kWh for $WECC_g$ CA_d, and from 0.16 to 0.13 $/kWh for $WECC_g$ $WECC_d$). Furthermore, the relative difference in system costs between CA_g CA_d and $WECC_g$ $WECC_d$ decreased when long-term storage was added to the grid. For a wind-solar-battery system, the relative difference in overall system cost between CA_g CA_d and $WECC_g$ $WECC_d$ was 16% whereas addition of PGP to the system resulted in a relative cost decrease of 13%. Meeting WECC electricity demand instead of California electricity demand with wind and solar resources over WECC ($WECC_g$ $WECC_d$ instead of $WECC_g$ CA_d) results in only very slight increases in overall system costs; $WECC_g$ $WECC_d$ costs are 1.06x that of $WECC_g$ CA_d without PGP and 1.04x with PGP. Using the same wind and solar resources as the $WECC_g$ CA_d scenario, the $WECC_g$ $WECC_d$ scenario reliably meets the demand of more people for a similar $/kWh cost.

To demonstrate how long-term planning affects least-cost systems, we include results for 1- to 6-year simulation lengths for both the CA_g CA_d and $WECC_g$ $WECC_d$ scenarios (Figure S6, Figure S7, Table S8, Table S9, Table S10, Table S11). We use a single year of demand data (2018) looped over the 39-year period from 1980 to 2018 and the historical wind and solar resource data for each year. This method does not capture the correlation between demand and weather data, but allows evaluation of the impact of weather variability against a representative demand year. Ultimately, the observations from the representative year (2018) are robust across multiple weather years, but the variability in results decreases with increased simulation length.

Geophysical and Siting Constraints on Installed Wind Capacity Raises System Costs, Increases the Importance of Long-Term Storage. As of 2019, California has about 6 GW of installed wind capacity.[66] When unconstrained, the least-cost system for CA_g CA_d with wind/solar generation and battery storage contained 90.9 GW of wind capacity, over an order of magnitude more than the currently installed capacity. The least-cost CA_g CA_d system with wind and solar generation as well as battery and PGP storage contained 67.7 GW of wind capacity. Realizing likely limitations on wind capacity that can be sited and deployed within the state of California, we therefore additionally ran optimizations over a range of specified wind capacities, allowing the other

https://doi.org/10.1021/acs.est.0c07848
Environ. Sci. Technol. XXXX, XXX, XXX−XXX

technologies (solar, batteries, and, when included, PGP) to be optimally deployed without constraint. As shown in Figure 5,

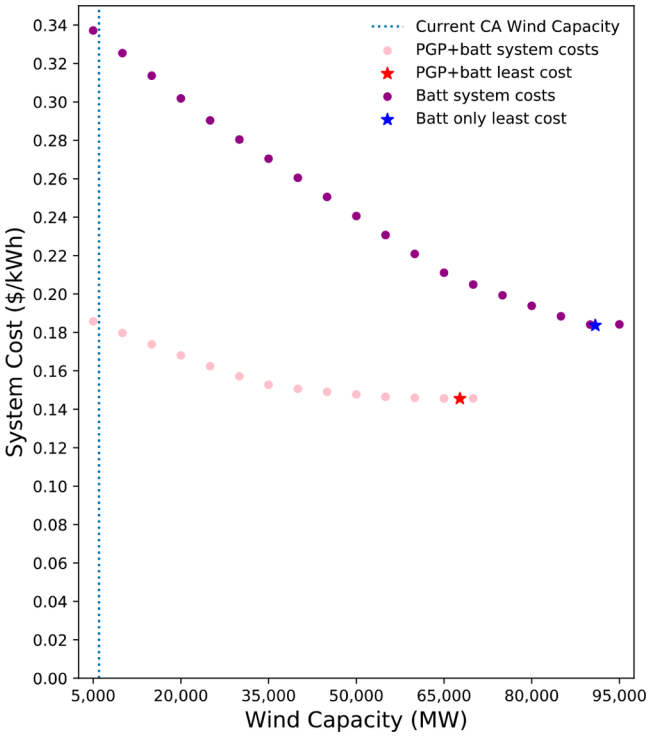

Figure 5. System cost for optimized systems with specified wind capacities. Each point shows the total system cost for a least-cost system using CA wind and solar generation sources and CA electricity demand with (pink) PGP storage and without (purple) PGP storage. Wind capacity was specified for each optimization but other resources (solar, batteries, PGP) were optimized to minimize cost. The vertical dashed line shows the current installed wind capacity in the state of California. The blue (battery storage only) and red (battery and PGP storage) stars mark the installed wind capacity and resulting total system costs for least-cost systems without any constraints. See Table S12 for the installed solar capacity and % wind capacity of total generation capacity for each optimization

lower specified wind capacities led to increases in overall system costs at the specified (100%) level of reliability. For a system with 10 GW of installed wind capacity, the overall system costs for optimizations with and without PGP were 0.18 and 0.33 $/kWh, respectively. For comparison, least-cost unconstrained systems with or without PGP (Figure 4) had costs of 0.15 and 0.18 $/kWh, respectively. Moreover, as installed wind capacities were more tightly constrained, the difference in system cost increased between systems with and without PGP; systems with both PGP and battery storage had substantially lower system costs than those with only batteries.

DISCUSSION

Analytical Assessment of the Variability of Wind and Solar Resources. Rare but extreme weather-related events as well as seasonal and interannual resource variability are critical features in determining the cost and asset deployment implementation of a highly reliable variable renewable electricity system. Over a 39-year period from 1980 to 2018 in California, resource droughts, defined as generation at less than half the expected mean for that day of year, were experienced on ∼2% of days for solar and ∼13% of days for wind. The passing of clouds will occasionally reduce solar generation, whereas this analytical assessment demonstrates that over a 4-decade time period, extensive cloud cover is present over essentially the entire state of California for episodes that can span multiple consecutive days. Some of these drought events occur consecutively, with the longest wind drought in California lasting 10 days. This run of days with low variable renewable generation poses a substantial challenge to the ability of system operators to ensure the requisite resource adequacy without extensive curtailment. Electricity dispatch over a 5-day wind drought in 2018 shows that, for a wind-solar-battery system, excess generation from solar generation is used to charge batteries to meet electricity demand. When long-duration storage is added, the least-cost system dispatches long-duration storage to meet electricity demand during this period of low wind resource (Figure S5). This analysis of these low-power periods, based off of multiple decades of historical weather data, provides a quantitative understanding of the dynamics of these resources, which can then inform asset deployment to ensure resource adequacy even in the face of extreme weather events.

Although marginal capacity expansion costs of solar electricity in California are currently competitive with electricity derived from natural gas, a highly reliable system based on solar generation constrained to be located fully within California in conjunction with battery storage was the most expensive option of all of the systems considered in this study (Figure S8). Several factors contribute to these high costs including (a) the need to overbuild, and consequently curtail, large amounts of electricity due to the seasonal variability in the solar resources (between summer and winter) that cannot be readily compensated for with short-term battery storage; (b) multiday solar droughts when the entire state of California is mostly or nearly entirely cloud-covered during daytime; (c) the expense associated with the large required energy capacity of battery storage that would be used very infrequently to provide reliability during such solar droughts. Few such solar droughts were present over the entire WECC, and none were present over CONUS. However, even over CONUS, the relatively high costs associated with 12 h of battery storage to compensate for diurnal variability of the solar resource produced relatively high electricity costs for reliable solar-battery systems, in conjunction with extensive curtailment associated with the seasonable variability of the solar resource.[25]

Caveats, Assumptions, and Limitations of the Macro Energy Model. To determine cost-effective solutions to meet electricity demand in a wind and solar generation electricity system, we employ a Macro Energy Model that optimizes deployment of generation and storage assets with perfect foresight, perfectly efficient markets, and no transmission losses. Although the target year for SB100 is 2045,[6] we use estimated current asset costs rather than projected future costs to allow for a direct comparison of how geographic constraints and resource variability impact system costs under otherwise constant cost assumptions. We assume free transmission without constraints, thereby excluding the trade-off between resource quality and transport cost in determining least-cost solutions.[67,68] Regardless of costs, expansion of transmission faces additional barriers such as siting or public opposition.[69,70] We exclude all of these potential barriers from consideration in this study.

https://doi.org/10.1021/acs.est.0c07848
Environ. Sci. Technol. XXXX, XXX, XXX−XXX

For the drought analysis, the results are based on historical weather data and do not account for potential future changes in resource variability resulting from climate change. Both more predictable, systemic changes in resource variability due to climate change, such as increased seasonal variability in the wind resource, and unpredictable events, such as climate-induced wildfires like those experienced in August through October 2020 where large fractions of California experienced substantial decreases in the daily solar resource due to smoke and haze, may occur. The frequency of these episodes in the future cannot be robustly predicted, so we explore solutions based on past performance to build a system that has an asset lifetime on the grid of many decades. In terms of electricity demand, our analysis reveals substantial gaps between variable renewable energy generation and load. Projections indicate that California electricity demand is expected to increase by ~11% in the highest demand scenario by 2030[71] and will most likely continue to increase by 2050 as various sectors are electrified. Therefore, the representative demand year used herein underestimates expected electricity demand in the future. Flexibility in electrification via technologies like vehicle-to-grid may help smooth variability from wind and solar resources[72] but faces severe challenges to fully compensate for the actual degree and duration of low-resource periods quantified herein or the daily, seasonal, and interannual variability of wind and solar generation. Ultimately, this increase in demand will only further exacerbate the challenge of ensuring grid reliability in a system dominated by variable renewable generation primarily from wind and solar resources. The bulk of the modeling results are from a single, representative year of wind and solar capacities and electricity demand data (2018). However, we also include analysis over 1-, 2-, 3-, 4-, 5-, and 6-year optimizations over the 39-year period to capture variation due to weather related events (Figure S6, Figure S7, Table S8, Table S9, Table S10, Table S11).

Our results are intended to help inform more detailed analyses of energy system options by highlighting factors that can substantially affect the cost of systems with high amounts of wind and solar generation. Some aspects of the analysis, such as the usefulness of long-duration storage to reduce system costs, are applicable to larger regions like CONUS,[25] but the availability of resources is specific to the region of interest. For example, the Western Interconnect includes both high-quality solar regions of the Southwestern US and high-quality wind regions of the Midwest, whereas regions like the Northeast or states like Florida do not have access to comparable resources.[68]

Grid Expansion as a Tool to Address Variability. Grid expansion offers a potential opportunity for smaller geographical regions, like California, to ameliorate some of the issues associated with in-state resource variability and availability, primarily associated with the wind resource (Figure 1). Aggregation of wind and solar resources over larger geographical areas reduces the variability of their generation profiles and minimizes the frequency and duration of resource droughts.[13] Furthermore, sharing of resources has been shown to reduce system costs in highly renewable energy systems in both Europe[72] and North America.[73] Studies that examine future electricity scenarios for the United States often incorporate such transmission expansion into their models to meet renewable electricity and/or CO_2 emissions restrictions requirements.[74,75] Large-scale transmission expansions may have minimal impacts on total system costs due to their small contribution to the overall cost of electricity, but potential siting and cost allocation limitations could severely impede these infrastructure developments.[22] Nevertheless, the potential system cost reductions and smoothing of resource variability afforded by transmission expansion make it essential to explore. Moreover, along with California, three other states in WECC (Nevada,[5] Washington,[12] and New Mexico[11]) have enacted legislative targets that by 2045 require construction and operation of 100% renewable and/or zero-carbon electricity systems.

Expansion of the transmission grid such that wind and solar resources are aggregated over WECC instead of CA would allow the entire region to benefit from decreased occurrences in resource droughts (Figure 2, Figure S2, Table S1, Figure S3, Table S2, Table S3, Table S4, Table S5). When comparing resources between CA and WECC, CA experienced about 16x and 2.6x more days of solar and wind droughts, respectively, than WECC over the 39-year record. Furthermore, of the drought days, the average duration of consecutive days for solar and wind droughts was 1.2 and 1.6 for CA compared to 1.1 and 1.4 for WECC, respectively. Additionally, wind and solar droughts occurred simultaneously on 27 days over the 39-year period when resources were restricted to be aggregated solely over CA, compared to only 6 days in WECC. With optimization to meet electricity demand using current technology costs for electricity systems with wind and solar generation, $/kWh system costs for larger regions ($WECC_g$ $WECC_d$) were lower than for smaller regions (CA_g CA_d) with or without deployment of long-term storage (Figure 4). Further cost reductions occurred when resources were aggregated over even larger areas such as CONUS (dotted line in Figure 4).

Long-Term Storage as a Tool to Address Gaps between Supply and Demand Due to Resource Variability. Although expansion of transmission infrastructure may reduce system costs and the effects of variability in wind and solar generation profiles, grid expansion faces potential siting and cost allocation barriers and requires coordination between decision-makers.[22,24] Even grid expansion over CONUS is not sufficient to eliminate resource variability to levels that would allow compliance with resource adequacy planning requirements without extensive curtailment of generation.[13] Addition of long-term storage has been shown to reduce system costs in wind- and solar-based electricity systems for CONUS and may face fewer logistical barriers to actualize regionally.[25] Here, we represent long-term storage as PGP with fuel cells and electrolyzers for power conversion, and hydrogen stored in underground salt caverns for energy storage. Various technological options for PGP storage, including the use of depleted geological reservoirs for underground storage and the repurposing of natural gas pipelines, could potentially provide additional flexibility and further reduce overall system costs. PGP costs are much more sensitive to reductions in power costs than hydrogen storage costs, due to the very low cost of energy storage as hydrogen gas either in tanks, caverns, or geological reservoirs, so the results are robust with respect to the cost of hydrogen storage.[25,43,76]

For all scenarios considered, addition of long-term storage, even at current estimated power-to-gas-to-power costs, reduced overall system costs for highly reliable systems based on variable renewable resources (Figure 4). For scenarios

https://doi.org/10.1021/acs.est.0c07848
Environ. Sci. Technol. XXXX, XXX, XXX−XXX

where California used in-state resources to meet its electricity demand (CA_g CA_d), addition of long-term storage to a wind-solar-battery electricity system reduced VRE curtailment from 72% of VRE generation on average (i.e., 12% of VRE capacity) to 8% of VRE generation on average (i.e., 2% of VRE capacity). Additionally, the system cost reductions due to grid expansion for systems with long-term storage were smaller than those for systems that did not have long-term storage, i.e., the relative difference between the cost per kWh for California (CA_g CA_d) and WECC ($WECC_g$ $WECC_d$) was smaller for systems that included long-term storage compared to systems that only relied on battery storage.

The least-cost system in which WECC wind and solar resources and battery storage were used to meet California demand ($WECC_g$ CA_d) contained substantial contributions from out-of-state wind and solar generation (Figure 4). In contrast, when long-term storage was included in the least-cost system, cost contributions from out-of-state wind decreased and only in-state solar generation was deployed. Dispatch curves over the optimization period (2018) demonstrate the roles of each of these technologies in such a system (Figure S9). With only wind/solar/battery storage deployed, out-of-state wind and solar generation was dispatched throughout the year to meet California electricity demand. However, when long-duration storage was included, excess in-state wind- and solar-generation and out-of-state wind-generation is used to charge the long-term storage, which would then be dispatched to meet increased demand during the summer months. Essentially, the long-term storage time-shifts a large portion of the electricity demand, thereby obviating the need for out-of-state solar generation. This finding indicates that long-term storage has the potential to reduce overall system costs for least-cost variable renewable resource-based electricity systems and additionally offers potential to reduce California's need to invest in out-of-state infrastructure while meeting its in-state electricity needs.

System Sensitivity to Constrained or Supplemental Generation. As of 2019, California has about 6 GW of installed wind capacity, with the majority of installed wind turbines in six main regions: Altamont, East San Diego County, Pacheco, Solano, San Gorgonio, and Tehachapi.[66,77] Although offshore wind technology could supplement onshore wind generation on the Eastern coast of the United States,[78] development of this resource in California is impeded by the steep coastline, siting restrictions, and potential objections from the military.[79,80] When unconstrained, the least-cost highly reliable system for CA_g CA_d with wind/solar generation and battery storage contained 90.9 GW of wind capacity, whereas the least-cost highly reliable system with wind/solar generation as well as battery and PGP storage contained 67.7 GW of wind capacity. At low specified wind capacities, systems with battery storage are nearly 2x more expensive than those that also deployed PGP, further emphasizing the cost-effectiveness of long-term storage as a tool to overcome variability in situations where California relies on its own wind and solar resources.

Although natural gas with carbon capture and sequestration (CCS) is not at present allowed within the legal framework of California Senate Bill 100,[20] we also explored the implications of including gas with CCS in the generation mix (Figure S10, Figure S11). In general, addition of low-cost fossil fuels, such as natural gas, to the generation mix minimizes or eliminates the need for long-term storage. However, the equipping of dispatchable natural gas generators with CCS increases capital costs.[46] Nevertheless, our results demonstrate that natural gas with CCS, with annual dispatch limited to 20% of total demand, can reduce costs in wind-solar-battery-PGP systems for all regions evaluated (Figure S10). Gas with CCS minimizes the need for long-term storage, even when gas with CCS is only included in the technology mix at 10% of demand (Figure S11), and completely eliminates long-term storage from the least-cost system at 20% of demand (Figure S10). Considerations of natural gas with CCS are important when considering the milestone of 60% carbon-free electricity in California by 2030, as the infrastructure necessary to meet this requirement may greatly differ from the deployment required for the end-state of 100% variable renewable electricity that we examined herein.

Water is an extremely constrained resource in California.[10] Nevertheless, about 11% of in-state generation in California in 2018 came from large hydroelectric generation.[81] Although only small hydroelectricity generation facilities technically fall under the category of renewable generation according to California's Renewable Portfolio Standards,[82] we additionally examined how addition of hydroelectric generation to a wind-solar-battery-PGP system would affect the asset mix of a least-cost electricity system. Historical hydroelectricity dispatch from the California Independent System Operator (CISO) from July 2018−July 2019 was subtracted from the California electricity demand (Figure S12), and the resulting system was optimized with respect to other storage and generation technologies to reliably meet the resulting demand profile. The addition of hydroelectricity at present levels in California had a minimal effect on overall system costs (at 0.14 $/kWh without and 0.13 $/kWh with hydro, assuming free hydro generation), and it shifted, only slightly, the technology mix in the least-cost system, with an increase in installed capacity of PGP from ∼14 days of mean CA demand to ∼15 days of mean CA demand and a decrease in installed capacity of batteries from ∼5.5 h of mean CA demand to 4.7 h of mean CA demand, for scenarios without and with hydro generation, respectively (Figure S13). Ultimately, the addition of hydroelectricity did not have substantial effects on either the system cost or technology mix in a least-cost electricity system, and moreover, the seasonality of hydroelectricity, which is most available in the spring, led to a slight increase in the absolute amount of the installed PGP capacity in reliable, least-cost variable renewable electricity-dominated systems.

Additional Means of Achieving Grid Reliability and Flexibility. Here, we explore multiple options to ensure reliability in a wind- and solar-based electricity system for California including transmission expansion, addition of long duration storage, and addition of supplemental generation in the form of natural gas with CCS and hydroelectricity. Additional forms of supplemental generation that we have not considered herein include geothermal, biomass, and concentrated solar power with thermal energy storage. These technologies may compete with natural gas on cost and flexibility limitations for generation but fill the same functional role as a flexible generation source, so we only evaluate scenarios with natural gas to determine the impact that flexible generation may have on the performance of the systems under evaluation. Other proposed options to increase flexibility and reliability of the electricity grid include expansion of the use of electricity to include sectors like heating and transportation, as well as demand management. More tightly coupled electricity,

https://doi.org/10.1021/acs.est.0c07848
Environ. Sci. Technol. XXXX, XXX, XXX−XXX

heating, and transportation sectors could decrease the need for and benefits of transmission expansion.[72] Although electrification of the heating sector would lead to increases in California winter electricity demand, these increases would still not match that of peak summer demand levels.[83] Therefore, the necessity of long-duration storage to compensate for this seasonal variability remains. In regard to transportation, we expect that deployed batteries in the form of a vehicle-to-grid scenario will have restrictions similar to those of the stationary batteries explored in this study when dealing with the multiday resource droughts that occur in both solar and wind generation. Similarly, the magnitude and duration of the deficit in wind- and solar-generation due to the long-duration resource droughts quantified in Figure 2 is too large to be easily accounted for with techniques like demand management.

■ ASSOCIATED CONTENT

Supporting Information

The Supporting Information is available free of charge at https://pubs.acs.org/doi/10.1021/acs.est.0c07848.

Model formulation, temporal variability of CONUS resources, results for different drought cutoffs, full tabulated results from droughts analysis, percent demand met for CONUS, dispatch over drought periods for CA, dispatch for $WECC_g$-CA_d scenario, system costs for systems with different technology mixes including natural gas with CCS, example energy storage for scenarios including hydroelectric generation, and a map of the regions used to generate resource data sets (PDF)

■ AUTHOR INFORMATION

Corresponding Author

Nathan S. Lewis − *Division of Chemistry and Chemical Engineering, California Institute of Technology, Pasadena, California 91125, United States;* orcid.org/0000-0001-5245-0538; Email: nslewis@caltech.edu

Authors

Katherine Z. Rinaldi − *Division of Chemistry and Chemical Engineering, California Institute of Technology, Pasadena, California 91125, United States;* orcid.org/0000-0002-0746-2852

Jacqueline A. Dowling − *Division of Chemistry and Chemical Engineering, California Institute of Technology, Pasadena, California 91125, United States*

Tyler H. Ruggles − *Department of Global Ecology, Carnegie Institution for Science, Stanford, California 94305, United States*

Ken Caldeira − *Department of Global Ecology, Carnegie Institution for Science, Stanford, California 94305, United States; Breakthrough Energy, Kirkland, Washington 98033, United States*

Complete contact information is available at: https://pubs.acs.org/10.1021/acs.est.0c07848

Notes

The authors declare no competing financial interest.

■ ACKNOWLEDGMENTS

This work was supported by fellowships at Caltech from SoCalGas in support of Low Carbon Energy Science and Policy, and by a gift from Gates Ventures LLC to the Carnegie Institution for Science. The authors thank Lei Duan and David J. Farnham for providing wind, solar, and demand input data.

■ REFERENCES

(1) DC Legislature. Clean Energy DC Omnibus Amendment Act of 2018; **2019**.

(2) Hawaii State Legislature. House Bill 623 Relating to Renewable Standards; **2015**.

(3) Virginia State Legislature. House Bill 1526 Virginia Clean Economy Act; **2020**.

(4) Maine State Legislature. Legislative Document 1494: An Act to Reform Maine's Renewable Portfolio Standard; **2019**.

(5) Nevada State Legislature. Nevada Senate Bill 358; **2019**.

(6) California State Legislature. Senate Bill 100: California Renewables Portfolio Standard Program: Emissions of Greenhouse Gases; **2018**.

(7) Legislative Assembly of Puerto Rico. Senate Bill 1121 Puerto Rico Energy Public Policy Act; **2019**.

(8) New York State Senate. Senate Bill S6599; **2019**.

(9) European Energy Commission. The European Green Deal; **2019**.

(10) International Renewable Energy Agency. Renewable Energy Target Setting. **2015**, 80.

(11) New Mexico State Legislature. Senate Bill 489: Energy Transition Act; **2019**.

(12) Carlyle, P.; McCoy, P.; Wellman, D.; Rolfes; Wilson, C.; Kuderer, N.; Keiser, L.; Hunt, S.; Darneille, B.Supporting Washington's Clean Energy Economy and Transitioning to a Clean, Affordable, Reliable Energy Future2020

(13) Shaner, M. R.; Davis, S. J.; Lewis, N. S.; Caldeira, K. Geophysical Constraints on the Reliability of Solar and Wind Power in the United States. *Energy Environ. Sci.* **2018**, *11* (4), 914−925.

(14) Collins, S.; Deane, P.; ÓGallachóir, B.; Pfenninger, S.; Staffell, I. Impacts of Inter-Annual Wind and Solar Variations on the European Power System. *Joule* **2018**, *2* (10), 2076−2090.

(15) Raynaud, D.; Hingray, B.; Franæois, B.; Creutin, J. D. Energy Droughts from Variable Renewable Energy Sources in European Climates. *Renewable Energy* **2018**, *125*, 578−589.

(16) Ohlendorf, N.; Schill, W.-P. Frequency and Duration of Low-Wind-Power Events in Germany. *Environmental Research Letters* **2020**, 15.

(17) Cannon, D. J.; Brayshaw, D. J.; Methven, J.; Coker, P. J.; Lenaghan, D. Using Reanalysis Data to Quantify Extreme Wind Power Generation Statistics: A 33 Year Case Study in Great Britain. *Renewable Energy* **2015**, *75*, 767−778.

(18) Weber, J.; Reyers, M.; Beck, C.; Timme, M.; Pinto, J. G.; Witthaut, D.; Schäfer, B. Wind Power Persistence Characterized by Superstatistics. *Sci. Rep.* **2019**, *9* (1), 19971.

(19) Collins, S.; Deane, P.; ÓGallachóir, B.; Pfenninger, S.; Staffell, I. Impacts of Inter-Annual Wind and Solar Variations on the European Power System. *Joule* **2018**, *2* (10), 2076−2090.

(20) California State Legislature. Senate Bill 100: California Renewables Portfolio Standard Program: Emissions of Greenhouse Gases; **2018**.

(21) California Energy Commission. Tracking Progress: Renewable Energy. **2018**.

(22) Jenkins, J. D.; Luke, M.; Thernstrom, S. Getting to Zero Carbon Emissions in the Electric Power Sector. *Joule* **2018**, *2* (12), 2498−2510.

(23) Sepulveda, N. A.; Jenkins, J. D.; de Sisternes, F. J.; Lester, R. K. The Role of Firm Low-Carbon Electricity Resources in Deep Decarbonization of Power Generation. *Joule* **2018**, *2* (11), 2403−2420.

(24) Ziegler, M. S.; Mueller, J. M.; Pereira, G. D.; Song, J.; Ferrara, M.; Chiang, Y.-M.; Trancik, J. E. Storage Requirements and Costs of Shaping Renewable Energy Toward Grid Decarbonization. *Joule* **2019**, *3* (9), 2134−2153.

(25) Dowling, J. A.; Rinaldi, K. Z.; Ruggles, T. H.; Davis, S. J.; Yuan, M.; Tong, F.; Lewis, N. S.; Caldeira, K. Role of Long-Duration Energy Storage in Variable Renewable Electricity Systems. *Joule* **2020**. 41907.
(26) Tarroja, B.; Peer, R. A. M.; SandersWind, K. T.; Grubert, E. How Do Non-Carbon Priorities Affect Zero-Carbon Electricity Systems? A Case Study of Freshwater Consumption and Cost for Senate Bill 100 Compliance in California. *Applied Energy* **2020**, *265*, 114824.
(27) Mahone, A.; Subin, Z.; Kahn-Lang, J.; Allen, D.; Li, V.; De Moor, G.; Ryan, N.; Price, S. *Deep Decarbonization in a High Renewables Future: Updated Results from the California PATHWAYS Model*. Sacramento, CA, 2018.
(28) Gueymard, C. A.; Wilcox, S. M. Assessment of Spatial and Temporal Variability in the US Solar Resource from Radiometric Measurements and Predictions from Models Using Ground-Based or Satellite Data. *Sol. Energy* **2011**, *85* (5), 1068−1084.
(29) Sengupta, M.; Xie, Y.; Lopez, A.; Habte, A.; Maclaurin, G.; Shelby, J. The National Solar Radiation Data Base (NSRDB). *Renewable Sustainable Energy Rev.* **2018**, *89*, 51−60.
(30) Li, X.; Zhong, S.; Bian, X.; Heilman, W. E. Climate and Climate Variability of the Wind Power Resources in the Great Lakes Region of the United States. *Journal of Geophysical Research: Atmospheres* **2010**, *115* (D18). DOI: 10.1029/2009JD013415.
(31) Brower, M. C.; Barton, M. S.; Lledó, L.; Dubois, J. A Study of Wind Speed Variability Using Global Reanalysis Data. **2013**.
(32) Kumler, A.; Carreño, I. L.; Craig, M. T.; Hodge, B.-M.; Cole, W.; Brancucci, C. Inter-Annual Variability of Wind and Solar Electricity Generation and Capacity Values in Texas. *Environ. Res. Lett.* **2019**, *14* (4), 044032.
(33) Rose, S.; Apt, J. What Can Reanalysis Data Tell Us about Wind Power? *Renewable Energy* **2015**, *83*, 963−969.
(34) Matsuo, Y.; Endo, S.; Nagatomi, Y.; Shibata, Y.; Komiyama, R.; Fujii, Y. Investigating the Economics of the Power Sector under High Penetration of Variable Renewable Energies. *Appl. Energy* **2020**, *267*, 113956.
(35) Handschy, M. A.; Rose, S.; Apt, J. Is It Always Windy Somewhere? Occurrence of Low-Wind-Power Events over Large Areas. *Renewable Energy* **2017**, *101*, 1124−1130.
(36) Williams, J. H.; DeBenedictis, A.; Ghanadan, R.; Mahone, A.; Moore, J.; Morrow, W. R.; Price, S.; Torn, M. S. The Technology Path to Deep Greenhouse Gas Emissions Cuts by 2050: The Pivotal Role of Electricity. *Science* **2012**, *335* (6064), 53.
(37) Morrison, G. M.; Yeh, S.; Eggert, A. R.; Yang, C.; Nelson, J. H.; Greenblatt, J. B.; Isaac, R.; Jacobson, M. Z.; Johnston, J.; Kammen, D. M.; Mileva, A.; Moore, J.; Roland-Holst, D.; Wei, M.; Weyant, J. P.; Williams, J. H.; Williams, R.; Zapata, C. B. Comparison of Low-Carbon Pathways for California. *Clim. Change* **2015**, *131* (4), 545−557.
(38) Colbertaldo, P.; Agustin, S. B.; Campanari, S.; Brouwer, J. Impact of Hydrogen Energy Storage on California Electric Power System: Towards 100% Renewable Electricity. *Int. J. Hydrogen Energy* **2019**, *44* (19), 9558−9576.
(39) North American Electric Reliability Corporation (NERC). 2012 State of Reliability, Technical Report.; **2012**.
(40) Ruggles, T. H.; Farnham, D. J.; Tong, D.; Caldeira, K. Developing Reliable Hourly Electricity Demand Data through Screening and Imputation. *Sci. Data* **2020**, *7* (1), 155.
(41) Levi, P. J.; Kurland, S. D.; Carbajales-Dale, M.; Weyant, J. P.; Brandt, A. R.; Benson, S. M. Macro-Energy Systems: Toward a New Discipline. *Joule* **2019**, *3* (10), 2282−2286.
(42) U.S. Energy Information Administration *Annual Energy Outlook*. U.S. Energy Information Administration 2018.
(43) Steward, D.; Saur, G.; Penev, M.; Ramsden, T. Lifecycle Cost Analysis of Hydrogen Versus Other Technologies for Electrical Energy Storage. *National Renewable Energy Lab (NREL)* **2009**.
(44) James, B.; Colella, W.; Moton, J.; Saur, G.; Ramsden, T. *PEM Electrolysis H2A Production Case Study Documentation*; Strategic A. Inc.: United States, 2013. DOI: 10.2172/1214980.
(45) Steward, D.; Penev, M.; Saur, G.; Becker, W.; Zuboy, J. Fuel Cell Power Model Version 2: Startup Guide, System Designs, and Case Studies. *Modeling Electricity, Heat, and Hydrogen Generation from Fuel Cell-Based Distributed Energy Systems*; NREL/TP-5600−57457, 1087789; 2013; p NREL/TP-5600−57457, 1087789. DOI: 10.2172/1087789.
(46) Davis, S. J.; Lewis, N. S.; Shaner, M.; Aggarwal, S.; Arent, D.; Azevedo, I. L.; Benson, S. M.; Bradley, T.; Brouwer, J.; Chiang, Y.-M.; Clack, C. T. M.; Cohen, A.; Doig, S.; Edmonds, J.; Fennell, P.; Field, C. B.; Hannegan, B.; Hodge, B.-M.; Hoffert, M. I.; Ingersoll, E.; Jaramillo, P.; Lackner, K. S.; Mach, K. J.; Mastrandrea, M.; Ogden, J.; Peterson, P. F.; Sanchez, D. L.; Sperling, D.; Stagner, J.; Trancik, J. E.; Yang, C.-J.; Caldeira, K. Net-Zero Emissions Energy Systems. *Science* **2018**, *360* (6396), No. eaas9793.
(47) Penev, M.; Saur, G.; Hunter, C.; Zuboy, J. H2A Hydrogen Production Model: Version 3.2018 User Guide (DRAFT). 68.
(48) Wilson, M. Lazard's Levelized Cost of Storage Analysis—Version 4.0. 60.
(49) Pellow, M. A.; Emmott, C. J. M.; Barnhart, C. J.; Benson, S. M. Hydrogen or Batteries for Grid Storage? A Net Energy Analysis. *Energy Environ. Sci.* **2015**, *8* (7), 1938−1952.
(50) Crotogino, F.; Donadei, S.; Bünger, U.; Landinger, H. *Large-Scale Hydrogen Underground Storage for Securing Future Energy Supplies* **2010**, *78*, 37−45.
(51) Gelaro, R.; McCarty, W.; Suárez, M. J.; Todling, R.; Molod, A.; Takacs, L.; Randles, C. A.; Darmenov, A.; Bosilovich, M. G.; Reichle, R.; Wargan, K.; Coy, L.; Cullather, R.; Draper, C.; Akella, S.; Buchard, V.; Conaty, A.; da Silva, A. M.; Gu, W.; Kim, G.-K.; Koster, R.; Lucchesi, R.; Merkova, D.; Nielsen, J. E.; Partyka, G.; Pawson, S.; Putman, W.; Rienecker, M.; Schubert, S. D.; Sienkiewicz, M.; Zhao, B. The Modern-Era Retrospective Analysis for Research and Applications, Version 2 (MERRA-2). *J. Clim.* **2017**, *30* (14), 5419−5454.
(52) Braun, J. E.; Mitchell, J. C. Solar Geometry for Fixed and Tracking Surfaces. *Sol. Energy* **1983**, *31* (5), 439−444.
(53) Meeus, J. H. *Astronomical Algorithms*; Willmann-Bell, Incorporated, 1991.
(54) Perez, R.; Ineichen, P.; Seals, R.; Michalsky, J.; Stewart, R. Modeling Daylight Availability and Irradiance Components from Direct and Global Irradiance. *Sol. Energy* **1990**, *44* (5), 271−289.
(55) Reindl, D. T.; Beckman, W. A.; Duffie, J. A. Diffuse Fraction Correlations. *Sol. Energy* **1990**, *45* (1), 1−7.
(56) Pfenninger, S.; Staffell, I. Long-Term Patterns of European PV Output Using 30 Years of Validated Hourly Reanalysis and Satellite Data. *Energy* **2016**, *114*, 1251−1265.
(57) Huld, T.; Gottschalg, R.; Beyer, H. G.; Topič, M. Mapping the Performance of PV Modules, Effects of Module Type and Data Averaging. *Sol. Energy* **2010**, *84* (2), 324−338.
(58) Bett, P. E.; Thornton, H. E. The Climatological Relationships between Wind and Solar Energy Supply in Britain. *Renewable Energy* **2016**, *87*, 96−110.
(59) United States Energy Information. Capacity factors for utility scale generators primarily using non fossil fuels, tech. rep. https://www.eia.gov/electricity/monthly/epm_table_grapher.php (accessed Sep 28, 2020).
(60) United States Energy Information. Hourly and daily balancing authority operations report data format and transmittal instructions EIA-930 https://www.eia.gov//Survey/index.php (accessed Sep 30, 2020).
(61) United States Energy Information. EIA-930 Data Users Guide and Known Issues. **2018**, 11.
(62) Ruggles, T. H.; Farnham, D. J. EIA Cleaned Hourly Electricity Demand Data, **2020**. DOI: 10.5281/zenodo.3690240.
(63) Lazard. Levelized Cost of Energy Analysis-Version 13.0 http://www.lazard.com/perspective/levelized-cost-of-energy-and-levelized-cost-of-storage-2019/ (accessed Sep 30, 2020).
(64) NREL (National Renewable Energy Laboratory). 2020 Annual Technology Baseline. **2020**.
(65) United States Energy Information. Annual Energy Outlook 2020 https://www.eia.gov/outlooks/aeo/ (accessed Sep 30, 2020).

https://doi.org/10.1021/acs.est.0c07848
Environ. Sci. Technol. XXXX, XXX, XXX−XXX

(66) Nyberg, M. Electricity From Wind Energy Statistics and Data https://ww2.energy.ca.gov/almanac/renewables_data/wind/index_cms.php.
(67) Proost, S.; Thisse, J.-F. What Can Be Learned from Spatial Economics? *Journal of Economic Literature* **2019**, *57* (3), 575−643.
(68) Bistline, J.; Santen, N.; Young, D. The Economic Geography of Variable Renewable Energy and Impacts of Trade Formulations for Renewable Mandates. *Renewable Sustainable Energy Rev.* **2019**, *106*, 79−96.
(69) Jenkins, J. D.; Luke, M.; Thernstrom, S. Getting to Zero Carbon Emissions in the Electric Power Sector. *Joule* **2018**, *2* (12), 2498−2510.
(70) MacDonald, A. E.; Clack, C. T. M.; Alexander, A.; Dunbar, A.; Wilczak, J.; Xie, Y. Future Cost-Competitive Electricity Systems and Their Impact on US CO2 Emissions. *Nat. Clim. Change* **2016**, *6* (5), 526−531.
(71) Commission, C. E. 2019 IEPR Workshops, Notices and Documents https://www.energy.ca.gov/data-reports/reports/integrated-energy-policy-report/2019-integrated-energy-policy-report/2019-iepr (accessed Oct 1, 2020).
(72) Brown, T.; Schlachtberger, D.; Kies, A.; Schramm, S.; Greiner, M. Synergies of Sector Coupling and Transmission Reinforcement in a Cost-Optimised, Highly Renewable European Energy System. *Energy* **2018**, *160*, 720−739.
(73) Bistline, J. E. T.; Brown, M.; Siddiqui, S. A.; Vaillancourt, K. Electric Sector Impacts of Renewable Policy Coordination: A Multi-Model Study of the North American Energy System. *Energy Policy* **2020**, *145*, 111707.
(74) MacDonald, A. E.; Clack, C. T. M.; Alexander, A.; Dunbar, A.; Wilczak, J.; Xie, Y. Future Cost-Competitive Electricity Systems and Their Impact on US CO2 Emissions. *Nat. Clim. Change* **2016**, *6* (5), 526−531.
(75) Mai, T.; Hand, M. M.; Baldwin, S. F.; Wiser, R. H.; Brinkman, G. L.; Denholm, P.; Arent, D. J.; Porro, G.; Sandor, D.; Hostick, D. J.; Milligan, M.; DeMeo, E. A.; Bazilian, M. Renewable Electricity Futures for the United States. *IEEE Transactions on Sustainable Energy* **2014**, *5* (2), 372−378.
(76) Schoenung, S. Economic Analysis of Large-Scale Hydrogen Storage for Renewable Utility Applications. In *International Colloquium on Environmentally Preferred Advanced Power Generation*; Citeseer, 2011; p 8e10.
(77) Wind Energy in California https://www.energy.ca.gov/data-reports/california-power-generation-and-power-sources/wind-energy-california.
(78) Mills, A. D.; Millstein, D.; Jeong, S.; Lavin, L.; Wiser, R.; Bolinger, M. Estimating the Value of Offshore Wind along the United States' Eastern Coast. *Environ. Res. Lett.* **2018**, *13* (9), 094013.
(79) Trump officials address prospects and challenges of California offshore wind development https://www.utilitydive.com/news/boem-central-california-coast-offshore-wind-development/580940/ (accessed Aug 25, 2020).
(80) Musial, W.; Beiter, P.; Tegen, S.; Smith, A. *Potential Offshore Wind Energy Areas in California: An Assessment of Locations, Technology, and Costs*; National Renewable Energy Lab.(NREL), Golden, CO (United States), 2016.
(81) Commission, C. E. 2018 Total System Electric Generation https://www.energy.ca.gov/data-reports/energy-almanac/california-electricity-data/2018-total-system-electric-generation (accessed Aug 26, 2020).
(82) Enforcement Procedures for the Renewables Portfolio Standard for Local Publicly Owned Electric Utilities. 38.
(83) Mahone, A.; Li, C.; Subin, Z.; Sontag, M.; Mantegna, G.; Karolides, A.; German, A.; Morris, P. Residential Building Electrification in California Consumer Economics, Greenhouse Gases and Grid Impacts. **2019**.

https://doi.org/10.1021/acs.est.0c07848
Environ. Sci. Technol. XXXX, XXX, XXX−XXX

Supplementary Information for

Wind and solar resource droughts in California highlight the benefits of long-term storage and integration with the Western Interconnect

Katherine Z. Rinaldi[1], Jacqueline A. Dowling[1], Tyler H. Ruggles[2], Ken Caldeira[2*], Nathan S. Lewis[1*]

1. *Division of Chemistry and Chemical Engineering, California Institute of Technology, Pasadena, CA 91125, USA*
2. *Department of Global Ecology, Carnegie Institution for Science, Stanford, CA 94305, USA*

This supplementary file is 26 pages and includes 12 tables and 14 figures.

1. Model formulation

1.1 Nomenclature

Symbol	Unit	Description
g (superscript)	-	Generation technology (wind, solar)
v (superscript)	-	Energy conversion (electrolyzer, fuel cell)
s (superscript)	-	Energy storage (PGP storage, battery storage)
from s (superscript)	-	Discharge from energy storage
to s (superscript)	-	Charge to energy storage
t (subscript)	h	Time step, starting from 1 and ending at T
c_{capital}	\$/kW for generation or conversion \$/kWh for storage	(Overnight) capital cost
c_{fixed}	\$/kW/h for generation or conversion \$/kWh/h for storage	Fixed cost
$c_{\text{fixed O\&M}}$	\$/kW/yr	Fixed operating and maintenance (O&M) cost
c_{var}	\$/kWh	Variable cost
f	-	Capacity factor (generation technology)
h	h/year	Average number of hours per year
i	-	Discount rate
n	yrs	Project life
Δt	h	Time step size, i.e., 1 hour in the model
C	kW for generation or conversion kWh for storage	Capacity
D_t	kW	Dispatch at time step t
M_t	kWh	Demand at time step t
S_t	kWh	Energy remaining in storage at time step t
γ	1/yr	Capital recovery factor
δ	1/h	Storage decay rate, or energy loss per hour expressed as fraction of energy in storage
η	-	Storage charging efficiency
τ	h	Storage charging duration

1.2 Cost calculations

Fixed cost of generation and conversion technologies (wind, solar, electrolyzer, fuel cell):

$$c_{\text{fixed}}^{g,v} = \frac{\gamma c_{\text{capital}}^{g,v} + c_{\text{fixed O\&M}}^{g,v}}{h}$$

Fixed cost of energy storage (PGP storage, battery storage):

$$c_{\text{fixed}}^{s} = \frac{\gamma c_{\text{capital}}^{s}}{h}$$

Capital recovery factor:

$$\gamma = \frac{i(1+i)^n}{(1+i)^n - 1}$$

1.3 Constraints

Capacity:

$$C^{g,v,s} \geq 0 \qquad \forall g, v, s$$

Dispatch:

$$0 \leq D_t^g \leq C^g f_t^g \qquad \forall g, t$$
$$0 \leq D_t^v \leq C^v \qquad \forall v, t$$
$$0 \leq D_t^{\text{to } s} \leq \frac{C^s}{\tau^s} \qquad \forall s, t$$
$$0 \leq D_t^{\text{from } s} \leq \frac{C^s}{\tau^s} \qquad \forall s, t$$
$$0 \leq S_t^s \leq C^s \qquad \forall s, t$$
$$0 \leq D_t^{\text{from } s} \leq S_t^s(1-\delta^s) \qquad \forall s, t$$

Storage energy balance:

$$S_1 = (1-\delta^s)S_t\Delta t + \eta^s D_T^{\text{to } s}\Delta t - D_T^{\text{from } s}\Delta t \qquad \forall s$$
$$S_{t+1} = (1-\delta^s)S_t\Delta t + \eta^s D_t^{\text{to } s}\Delta t - D_t^{\text{from } s}\Delta t \qquad \forall s, t \in 1, \ldots, (T-1)$$

System energy balance:

$$\sum_g D_t^g \Delta t + D_t^{\text{from } s}\Delta t = M_t + D_t^{\text{to } s}\Delta t \qquad \forall g, t$$

1.4 Objective function

$$minimize(system\ cost)$$

$$system\ cost = \sum_g c_{fixed}^g C^g + \sum_g \left(\frac{\sum_t c_{var}^g D_t^g}{T}\right) + \sum_v c_{fixed}^v C^v + \sum_s c_{fixed}^s C^s + \frac{\sum_t c_{var}^{to\ s} D_t^s}{T} + \frac{\sum_t c_{var}^{from\ s} D_t^s}{T}$$

2. *Supplementary figures and tables*

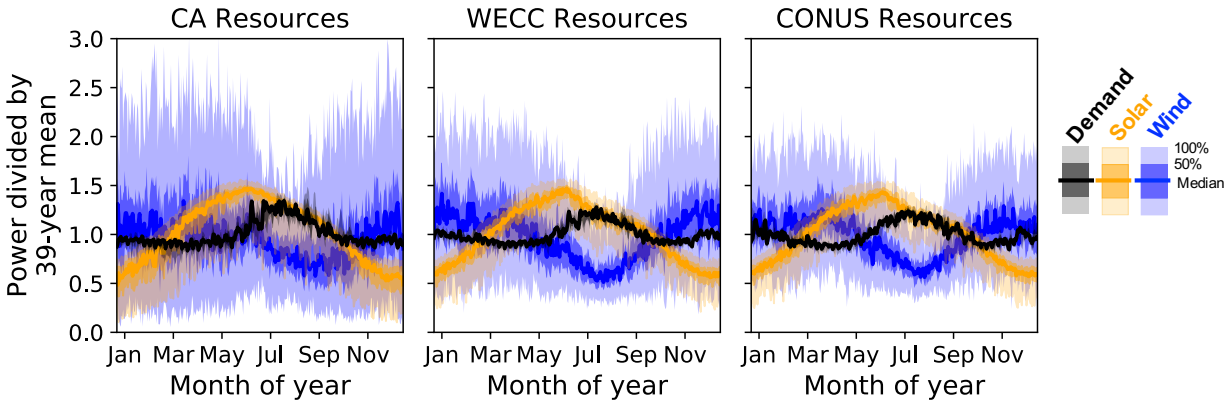

Figure S1: Temporal variability of wind (blue) and solar (yellow) resources over California, the Western Interconnect, and the contiguous U.S. during the 39-year period from 1980-2018. Seasonal variability of a single year (2018) of electricity demand (black). This figure is the same as Figure 1 with the addition of CONUS resources and demand. As in Figure 1, the dark line shows the median value and the darker and lighter shadings show the 25th to 75th and 0th to 100th percentiles of data, respectively. All data are normalized to their respective mean over the time period.

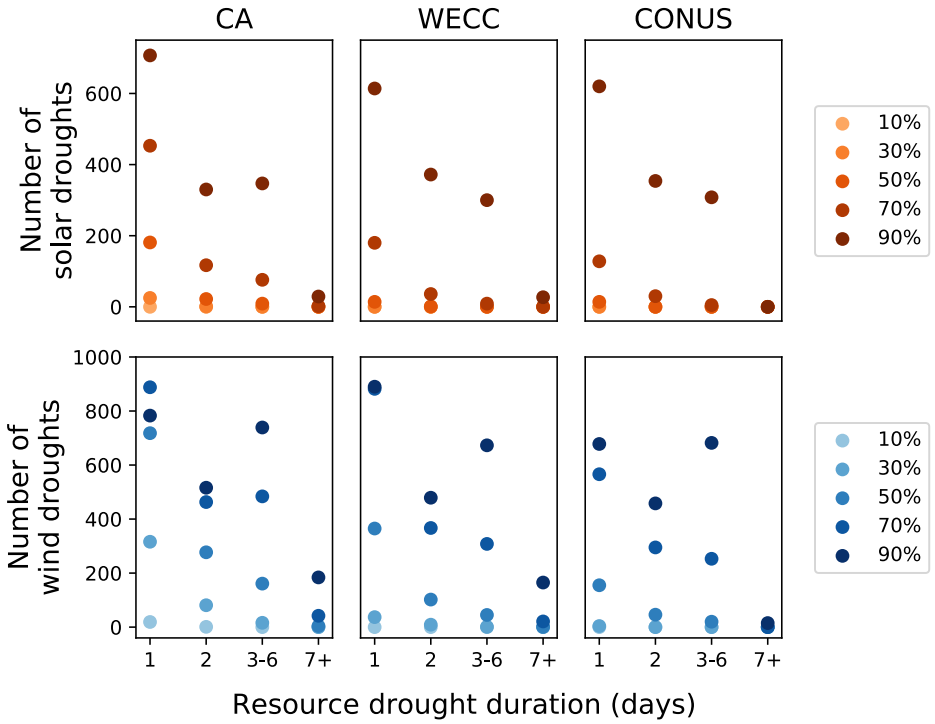

Figure S2: Resource droughts in California, the Western Interconnect, and the contiguous United States at for different threshold cutoffs. Each plot shows the number of instances where the mean daily capacity factor for solar (orange) and wind (blue) was less than the threshold percent of the mean daily capacity factor for that day of the year over the 39-year period for a duration of 1-, 2-, 3-6, or 7+ days. Resource droughts greater than 1-day in duration are not also counted toward 1-day occurrences. The threshold cutoffs are varied from 10% to 90% where darker dots indicate a higher threshold cutoff. The supporting data for this plot is in Table S1.

Wind Resource Droughts												
	1 day			2 days			3-6 days			7+ days		
	CA	WECC	CONUS	CA	WECC	CONUS	CA	WECC	CONUS	CA	WECC	CONUS
10%	19	0	0	1	0	0	0	0	0	0	0	0
30%	316	37	4	81	9	0	16	1	0	0	0	0
50%	718	365	155	277	102	46	161	45	20	4	1	0
70%	888	882	566	463	367	295	484	308	253	42	21	0
90%	783	890	678	516	479	458	739	673	682	184	165	15

Solar Resource Droughts												
	1 day			2 days			3-6 days			7+ days		
	CA	WECC	CONUS	CA	WECC	CONUS	CA	WECC	CONUS	CA	WECC	CONUS
10%	0	0	0	0	0	0	0	0	0	0	0	0
30%	25	0	0	1	0	0	0	0	0	0	0	0
50%	181	14	14	22	1	0	9	0	0	0	0	0
70%	453	180	128	117	36	30	76	9	5	2	0	0
90%	707	614	620	330	372	354	347	300	308	29	27	0

Table S1: Number of instances and duration of wind and solar resource droughts for California, the Western Interconnect, and the contiguous United States for different threshold cutoffs. Resource droughts are defined as days where the daily mean capacity factor is less than X% of the mean daily capacity factor for that day of the year over the 39-year period. Resource droughts greater than 1-day in duration are not also counted toward 1-day occurrences. This data is plotted in Figure S2.

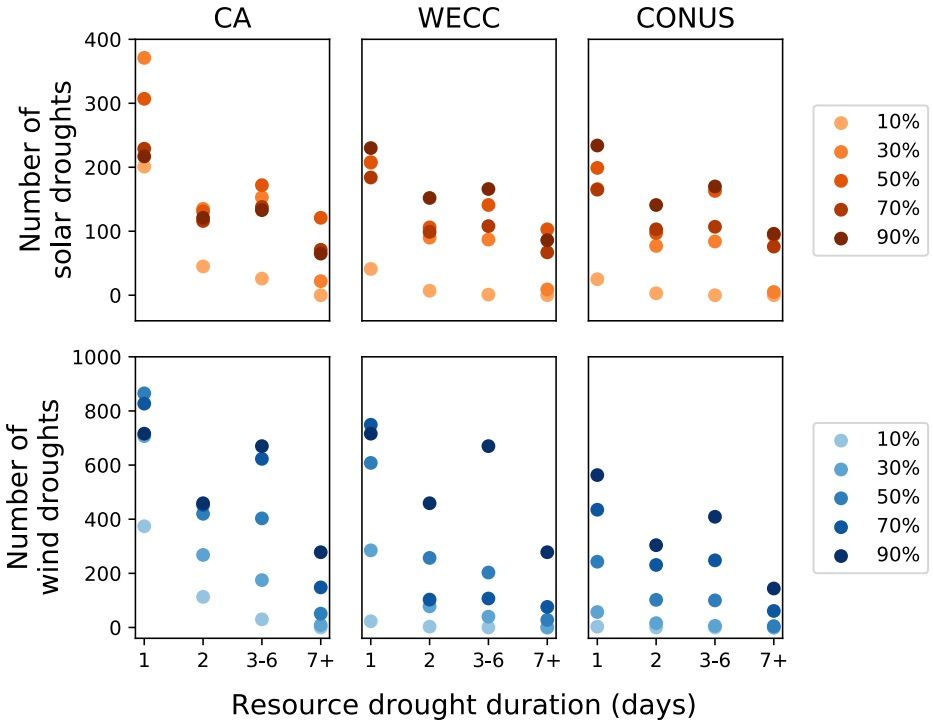

Figure S3: Resource droughts in California, the Western Interconnect, and the contiguous United States at for different capacity factor cutoffs. Each plot shows the number of instances where the mean daily capacity factor for solar (orange) and wind (blue) was less than the threshold capacity for a duration of 1-, 2-, 3-6, or 7+ days. Resource droughts greater than 1-day in duration are not also counted toward 1-day occurrences. The capacity factor cutoffs are varied from 10% to 30% where darker dots indicate a higher threshold cutoff. The supporting data for this plot is in Table S2.

Wind Resource Droughts												
	1 day			2 days			3-6 days			7+ days		
	CA	WECC	CONUS	CA	WECC	CONUS	CA	WECC	CONUS	CA	WECC	CONUS
10%	374	23	3	113	3	0	30	0	0	0	0	0
15%	707	285	57	268	78	16	175	40	6	9	0	0
20%	865	608	243	420	257	102	403	203	100	51	28	5
25%	827	749	435	453	103	231	623	107	248	148	76	61
30%	716	716	563	459	459	304	670	670	409	278	278	144

Solar Resource Droughts												
	1 day			2 days			3-6 days			7+ days		
	CA	WECC	CONUS	CA	WECC	CONUS	CA	WECC	CONUS	CA	WECC	CONUS
10%	201	41	25	45	7	3	26	1	0	0	0	0
15%	371	207	166	135	90	77	153	87	84	22	9	5
20%	307	208	199	131	106	97	172	141	163	121	103	94
25%	229	184	165	116	99	103	138	108	107	71	67	76
30%	217	230	234	121	152	141	133	166	170	65	86	96

Table S2: Number of instances and duration of wind and solar resource droughts for California, the Western Interconnect, and the contiguous United States for different threshold cutoffs. Resource droughts are defined as days where the daily mean capacity factor is less than X% of the mean daily capacity factor for that day of the year over the 39-year period. Resource droughts greater than 1-day in duration are not also counted toward 1-day occurrences. This data is plotted in Figure S2.

	Solar resource droughts			Wind resource droughts		
Drought duration (days)	CA	WECC	CONUS	CA	WECC	CONUS
1	181	14	14	718	365	155
2	22	1	0	277	102	46
3	7	0	0	94	33	14
4	1	0	0	44	5	4
5	0	0	0	16	5	1
6	1	0	0	7	2	1
7	0	0	0	2	1	0
8	0	0	0	1	0	0
9	0	0	0	0	0	0
10	0	0	0	1	0	0
Total drought days	256	16	14	1884	732	316

Table S3: Number of instances and duration of solar and wind resource droughts for California, WECC, and CONUS over the 39-year period from 1980-2018. Resource droughts are defined as days where the daily mean capacity factor is less than 50% of the mean daily capacity factor for that day of the year over the 39-year period. Resource droughts greater than 1-day in duration are not also counted toward 1-day occurrences.

SOLAR	1 day		2 days		3-6 days		7+ days	
Year	CA	WECC	CA	WECC	CA	WECC	CA	WECC
1980	4	2	1	0	0	0	0	0
1981	7	0	0	0	0	0	0	0
1982	12	0	3	0	0	0	0	0
1983	5	0	2	1	1	0	0	0
1984	0	1	0	0	0	0	0	0
1985	4	0	1	0	0	0	0	0
1986	5	1	0	0	0	0	0	0
1987	6	0	0	0	0	0	0	0
1988	2	1	0	0	1	0	0	0
1989	0	0	0	0	0	0	0	0
1990	0	0	0	0	0	0	0	0
1991	3	2	1	0	0	0	0	0
1992	7	1	0	0	0	0	0	0
1993	6	1	1	0	0	0	0	0
1994	4	0	0	0	0	0	0	0
1995	7	0	1	0	1	0	0	0
1996	7	0	2	0	1	0	0	0
1997	6	0	2	0	0	0	0	0
1998	8	0	1	0	0	0	0	0
1999	0	0	0	0	0	0	0	0
2000	7	0	1	0	1	0	0	0
2001	5	0	0	0	1	0	0	0
2002	1	0	0	0	0	0	0	0
2003	8	0	0	0	1	0	0	0
2004	5	0	1	0	0	0	0	0
2005	10	2	0	0	0	0	0	0
2006	6	0	1	0	0	0	0	0
2007	4	0	0	0	0	0	0	0
2008	2	0	2	0	0	0	0	0
2009	7	1	0	0	0	0	0	0
2010	3	0	0	0	2	0	0	0
2011	3	1	0	0	0	0	0	0
2012	4	0	0	0	0	0	0	0
2013	1	0	0	0	0	0	0	0
2014	5	0	0	0	0	0	0	0
2015	1	1	0	0	0	0	0	0
2016	4	0	1	0	0	0	0	0
2017	7	0	0	0	0	0	0	0
2018	5	0	1	0	0	0	0	0
median	5	0	0	0	0	0	0	0
mean	4.64	0.36	0.56	0.03	0.23	0	0	0
std	2.82	0.63	0.79	0.16	0.48	0	0	0
min	0	0	0	0	0	0	0	0
25%	3	0	0	0	0	0	0	0
50%	5	0	0	0	0	0	0	0
75%	7	1	1	0	0	0	0	0
max	12	2	3	1	2	0	0	0

Table S4: Solar drought events per year for CA and WECC. Solar droughts are defined as days where the daily mean capacity factor is less than 50% of the mean capacity factor for that day over the 39-year period from 1980-2018. This table supports Figure 2.

WIND	1 day		2 days		3-6 days		7+ days	
Year	CA	WECC	CA	WECC	CA	WECC	CA	WECC
1980	14	6	3	1	7	2	0	0
1981	17	12	5	6	3	0	0	1
1982	16	10	9	4	4	0	0	0
1983	21	10	6	5	2	2	0	0
1984	22	7	9	2	2	1	0	0
1985	22	5	4	3	3	3	1	0
1986	17	7	7	4	6	1	0	0
1987	15	14	8	4	11	3	0	0
1988	20	14	13	1	4	0	0	0
1989	16	6	3	5	4	0	0	0
1990	18	8	9	1	5	1	0	0
1991	19	9	8	0	2	1	0	0
1992	20	10	10	4	6	2	0	0
1993	16	11	10	2	3	1	0	0
1994	17	8	6	3	5	1	0	0
1995	21	14	9	3	3	2	1	0
1996	19	*6*	6	4	0	0	0	0
1997	19	16	6	3	2	1	0	0
1998	18	13	8	5	2	1	0	0
1999	22	6	6	1	3	0	0	0
2000	18	8	8	3	7	1	0	0
2001	21	11	5	4	2	3	0	0
2002	21	12	4	1	5	3	0	0
2003	18	12	5	2	7	2	0	0
2004	14	15	8	3	5	1	0	0
2005	25	9	6	8	5	2	0	0
2006	15	11	9	0	3	1	0	0
2007	15	11	13	2	4	1	0	0
2008	28	3	8	1	4	0	0	0
2009	12	6	7	3	4	0	0	0
2010	17	6	5	1	3	4	0	0
2011	19	5	6	1	3	0	0	0
2012	18	8	5	0	4	1	0	0
2013	17	8	6	2	6	0	0	0
2014	22	7	4	2	5	0	0	0
2015	21	11	7	3	8	3	1	0
2016	17	8	9	2	4	1	0	0
2017	16	7	9	2	2	0	1	0
2018	15	15	8	1	3	0	0	0
median	18	9	7	2	4	1	0	0
mean	18.41	9.36	7.10	2.62	4.13	1.15	0.10	0.03
std	3.20	3.25	2.36	1.76	2.07	1.11	0.31	0.16
min	12	3	3	0	0	0	0	0
25%	16	7	5.5	1	3	0	0	0
50%	18	9	7	2	4	1	0	0
75%	21	11.5	9	4	5	2	0	0
max	28	16	13	8	11	4	1	1

Table S5: Wind drought events per year for CA and WECC. Wind droughts are defined as days where the daily mean capacity factor is less than 50% of the mean capacity factor for that day over the 39-year period from 1980-2018. This table supports Figure 2.

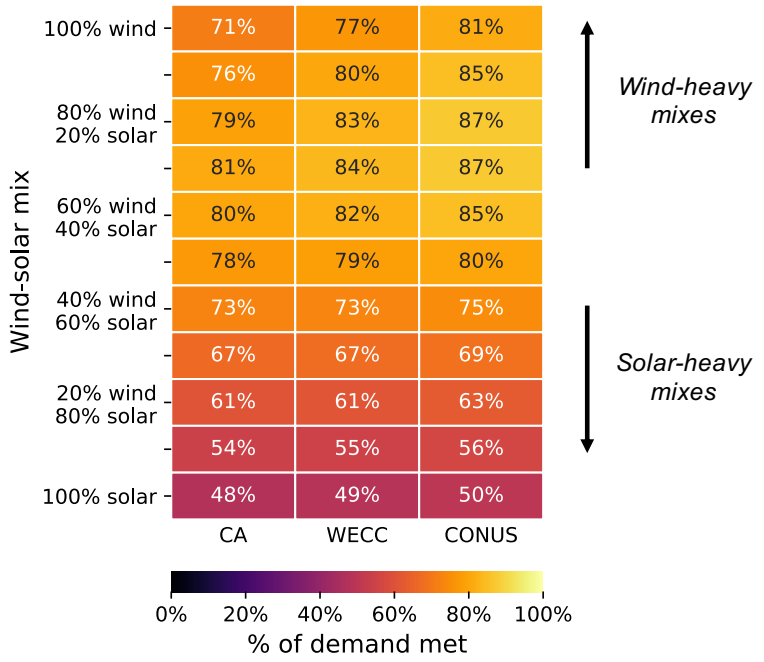

Figure S4: Percent demand met over the 39-year period from 1980-2018 for wind and solar based electricity systems. Each plot shows the potential of renewable resources to meet electricity demand for California (left column), the Western Interconnect (middle column), and the contiguous United States (right column). Each row corresponds to a different wind/solar generation mix. Marked percentages refer to the reliability (% of demand met) over the entire 39-year period for each region and mix.

Demand region	Generation region	Technology mix	Wind 1	Wind 2	Solar 1	Solar 2	PGP	Battery	Total system cost
CA	CA	wind 1, solar 1, battery	0.06	-	0.07	-	-	0.06	0.18
CA	WECC	wind 1, wind 2, solar 1, solar 2, battery	0.04	0.06	0.02	0.04	-	0.02	0.17
WECC	WECC	wind 1, solar 1, battery	0.07	-	0.05	-	-	0.03	0.16
CA	CA	wind 1, solar 1, battery, PGP	0.04	-	0.04	-	0.04	0.02	0.15
CA	WECC	wind 1, wind 2, solar 1, solar 2, battery, PGP	0.01	0.04	0.03	0.00	0.04	0.01	0.13
WECC	WECC	wind 1, solar 1, battery, PGP	0.05	0.00	0.03	-	0.04	0.01	0.13

Table S6: System cost contributions for technology mixes and geographical regions. This data table supports Figure 4. Rounded values in each technology column represent the cost contribution in $/kWh for that technology to the total system cost. Costs for PGP include both power-related and energy-related costs. Exact values, not the rounded values shown here, were used for secondary calculations. When included, wind 2 and solar 2 refer to the wind and solar resources from the rest of WECC (not including CA).

Demand region	Generation region	Technology mix	PGP input power capacity, electrolyzers (1 kW = mean demand)	PGP energy capacity (hours of mean demand)	PGP output power capacity, fuel cells (1 kW = mean demand)	Duration (hours)
CA	CA	wind 1, solar 1, battery, PGP	0.32	388.61	0.48	812.16
CA	WECC	wind 1, solar 1, wind 2, solar 2, battery, PGP	0.27	495.04	0.61	806.74
WECC	WECC	wind 1, solar 1, battery, PGP	0.26	423.73	0.51	832.41

Table S7: PGP energy and power capacities for technology mixes and geographical regions. Rounded values for the PGP input power capacity (electrolyzers), PGP energy capacity, and PGP ouput power capacity (fuel cells) are given for each geographical scenario. The values are in terms of mean demand from the specified demand region. This data table supports Figure 4.

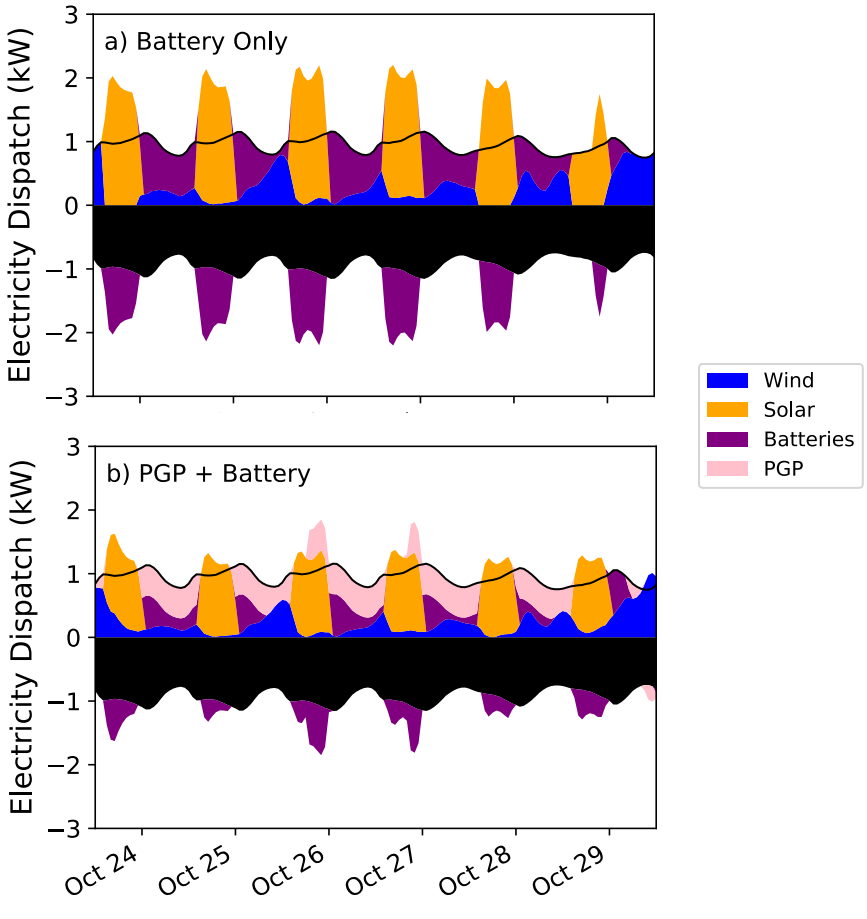

Figure S5: Electricity dispatch during a 5 day wind drought for the CA_g-CA_d case. Electricity sources (positive values) and sinks (negative values) to the grid are balanced for each hour during the optimization period (2018). Plots show the 5-day averaged results over a wind drought lasting from October 24 to October 29 for a system with battery storage only (a) and for a system with both PGP and battery storage (b). Generation sources (wind and solar) and dispatch from storage are balanced by end-use demand and charging of storage for each hour.

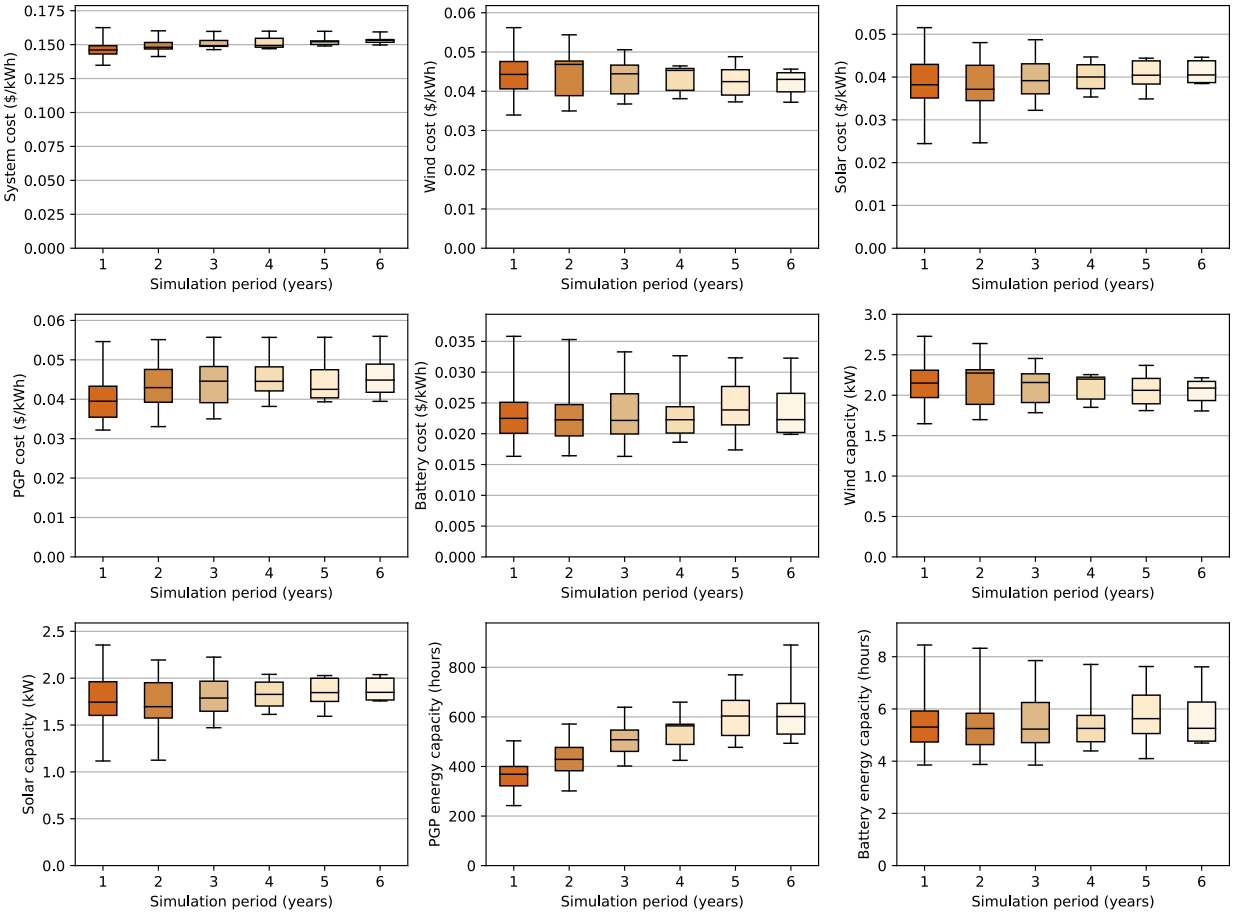

Figure S6: Distribution of results for the CA_g-CA_d scenario for various simulation lengths. Box and whisker plots show the distribution of system costs as well as the installed capacities and cost contributions for all storage and generation technologies over various simulation lengths (1- to 6-year lengths). Whiskers represent the minimum and maximum of each dataset. Power capacities are normalized such that 1 kW is mean CA demand and energy capacity is presented in hours of mean CA demand. Supporting data for this plot is in Table S8 and Table S9.

Simulation length (across 39 years, 1980-2018)	Data type	Wind power capacity (1 kW = mean CA demand)	Solar power capacity (1 kW = mean CA demand)	PGP energy capacity (hours of mean CA demand)	Battery energy capacity (hours of mean CA demand)
1-yr periods (start years: 1980, 1981, 1982, 1983, 1984, 1985, 1986, 1987, 1988, 1989, 1990, 1991, 1992, 1993, 1994, 1995, 1996, 1997, 1998, 1999, 2000, 2001, 2002, 2003, 2004, 2005, 2006, 2007, 2008, 2009, 2010, 2011, 2012, 2013, 2014, 2015, 2016, 2017, 2018)	Max Q3 Median Q1 Min spread	2.73 2.31 2.15 1.97 1.65 66.0 %	2.35 1.96 1.74 1.60 1.12 111.0 %	503.36 400.01 368.65 321.78 242.12 108.0 %	8.45 5.92 5.31 4.73 3.85 119.0 %
2-yr periods (start years: 1980, 1982, 1984, 1986, 1988, 1990, 1992, 1994, 1996, 1998, 2000, 2002, 2004, 2006, 2008, 2010, 2012, 2014, 2016, 2018)	Max Q3 Median Q1 Min spread	2.64 2.32 2.27 1.89 1.70 55.0 %	2.19 1.95 1.70 1.58 1.13 95.0 %	571.12 476.88 428.65 382.78 301.37 90.0 %	8.32 5.83 5.25 4.63 3.87 115.0 %
3-yr periods (start years: 1980, 1983, 1986, 1989, 1992, 1995, 1998, 2001, 2004, 2007, 2010, 2013, 2016)	Max Q3 Median Q1 Min spread	2.46 2.27 2.16 1.91 1.78 38.0 %	2.23 1.97 1.79 1.65 1.47 51.0 %	639.021 546.93 507.85 460.83 401.91 59.0 %	7.85 6.25 5.23 4.71 3.85 104.0 %
4-yr periods (start years: 1980, 1984, 1988, 1992, 1996, 2000, 2004, 2008, 2012, 2016)	Max Q3 Median Q1 Min spread	2.26 2.22 2.2 1.95 1.85 22.0 %	2.04 1.96 1.83 1.70 1.61 26.0 %	659.51 570.40 563.81 489.02 424.72 55.0 %	7.70 5.75 5.25 4.74 4.39 75.0 %
5-yr periods (start years: 1980, 1985, 1990, 1995, 2000, 2005, 2010, 2015)	Max Q3 Median Q1 Min spread	2.37 2.21 2.06 1.89 1.81 31.0 %	2.03 2.00 1.85 1.75 1.59 27.0 %	769.66 666.67 603.53 525.14 477.21 61.0 %	7.62 6.53 5.63 5.06 4.10 86.0 %
6-yr periods (start years: 1980, 1986, 1992, 1998, 2004, 2010, 2016)	Max Q3 Median Q1 Min spread	2.22 2.17 2.09 1.93 1.81 23.0 %	2.04 2.0 1.85 1.77 1.76 16.0 %	890.03 654.41 601.41 530.66 493.56 80.0 %	7.61 6.26 5.26 4.77 4.69 62.0 %

Table S8: Distribution of capacities for various simulation lengths for the CA_g CA_d scenario. This table supports Figure S5. Spread is defined as the relative difference between the max and the min: (max-min)/min x 100.

Simulation length (across 39 years, 1980-2018)	Data type	Total system cost ($/kWh)	Wind cost ($/kWh)	Solar cost ($/kWh)	PGP cost ($/kWh)	Battery cost ($/kWh)
1-yr periods (start years: 1980, 1981, 1982, 1983, 1984, 1985, 1986, 1987, 1988, 1989, 1990, 1991, 1992, 1993, 1994, 1995, 1996, 1997, 1998, 1999, 2000, 2001, 2002, 2003, 2004, 2005, 2006, 2007, 2008, 2009, 2010, 2011, 2012, 2013, 2014, 2015, 2016, 2017, 2018)	Max Q3 Median Q1 Min spread	0.163 0.149 0.146 0.143 0.135 21.0 %	0.056 0.048 0.044 0.041 0.034 66.0 %	0.052 0.043 0.038 0.035 0.024 111.0 %	0.055 0.043 0.04 0.035 0.032 70.0 %	0.036 0.025 0.022 0.02 0.016 119.0 %
2-yr periods (start years: 1980, 1982, 1984, 1986, 1988, 1990, 1992, 1994, 1996, 1998, 2000, 2002, 2004, 2006, 2008, 2010, 2012, 2014, 2016, 2018)	Max Q3 Median Q1 Min spread	0.16 0.152 0.148 0.147 0.141 13.0 %	0.054 0.048 0.047 0.039 0.035 55.0 %	0.048 0.043 0.037 0.034 0.025 95.0 %	0.055 0.048 0.043 0.039 0.033 67.0 %	0.035 0.025 0.022 0.02 0.016 115.0 %
3-yr periods (start years: 1980, 1983, 1986, 1989, 1992, 1995, 1998, 2001, 2004, 2007, 2010, 2013, 2016)	Max Q3 Median Q1 Min spread	0.16 0.153 0.149 0.149 0.146 9.0 %	0.051 0.047 0.044 0.039 0.037 38.0 %	0.049 0.043 0.039 0.036 0.032 51.0 %	0.056 0.048 0.045 0.039 0.035 59.0 %	0.033 0.026 0.022 0.02 0.016 104.0 %
4-yr periods (start years: 1980, 1984, 1988, 1992, 1996, 2000, 2004, 2008, 2012, 2016)	Max Q3 Median Q1 Min spread	0.16 0.155 0.149 0.148 0.147 9.0 %	0.046 0.046 0.045 0.04 0.038 22.0 %	0.045 0.043 0.04 0.037 0.035 26.0 %	0.056 0.048 0.045 0.042 0.038 46.0 %	0.033 0.024 0.022 0.02 0.019 75.0 %
5-yr periods (start years: 1980, 1985, 1990, 1995, 2000, 2005, 2010, 2015)	Max Q3 Median Q1 Min spread	0.16 0.153 0.152 0.15 0.149 7.0 %	0.049 0.045 0.042 0.039 0.037 31.0 %	0.044 0.044 0.04 0.038 0.035 27.0 %	0.056 0.047 0.043 0.04 0.039 42.0 %	0.032 0.028 0.024 0.021 0.017 86.0 %
6-yr periods (start years: 1980, 1986, 1992, 1998, 2004, 2010, 2016)	Max Q3 Median Q1 Min spread	0.159 0.154 0.153 0.152 0.15 6.0 %	0.046 0.045 0.043 0.04 0.037 23.0 %	0.045 0.044 0.04 0.039 0.038 16.0 %	0.056 0.049 0.045 0.042 0.039 42.0 %	0.032 0.027 0.022 0.02 0.02 62.0 %

Table S9: Distribution of cost contributions for various simulation lengths for the CA_g CA_d scenario. This table supports Figure S5. Spread is defined as the relative difference between the max and the min: (max-min)/min x 100.

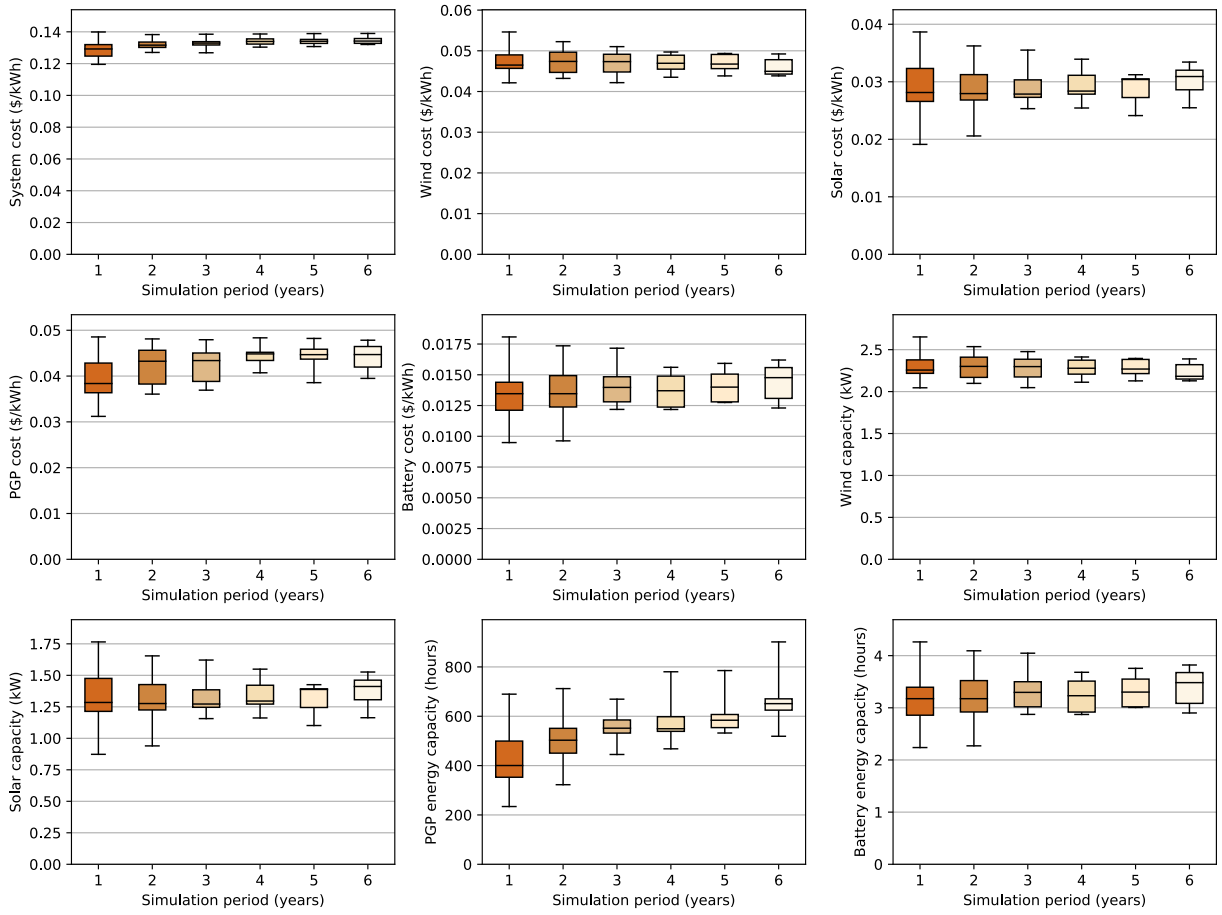

Figure S7: Distribution of results for the $WECC_g$ $WECC_d$ scenario for various simulation lengths. Box and whisker plots show the distribution of system costs as well as the installed capacities and cost contributions for all storage and generation technologies over various simulation lengths (1- to 6-year lengths). Whiskers represent the minimum and maximum of each dataset. Power capacities are normalized such that 1 kW is mean WECC demand and energy capacity is presented in hours of mean WECC demand. Supporting data for this plot is in Table S10 and Table S11.

Simulation length (across 39 years, 1980-2018)	Data type	Wind power capacity (1 kW = mean WECC demand)	Solar power capacity (1 kW = mean WECC demand)	PGP energy capacity (hours of mean WECC demand)	Battery energy capacity (hours of mean WECC demand)
1-yr periods (start years: 1980, 1981, 1982, 1983, 1984, 1985, 1986, 1987, 1988, 1989, 1990, 1991, 1992, 1993, 1994, 1995, 1996, 1997, 1998, 1999, 2000, 2001, 2002, 2003, 2004, 2005, 2006, 2007, 2008, 2009, 2010, 2011, 2012, 2013, 2014, 2015, 2016, 2017, 2018)	Max Q3 Median Q1 Min spread	2.65 2.38 2.26 2.22 2.05 30.0 %	1.77 1.48 1.29 1.21 0.87 102.0 %	689.59 499.43 400.34 352.82 234.09 195.0 %	4.26 3.39 3.18 2.86 2.24 90.0 %
2-yr periods (start years: 1980, 1982, 1984, 1986, 1988, 1990, 1992, 1994, 1996, 1998, 2000, 2002, 2004, 2006, 2008, 2010, 2012, 2014, 2016, 2018)	Max Q3 Median Q1 Min spread	2.54 2.41 2.3 2.17 2.10 21.0 %	1.65 1.43 1.28 1.23 0.94 76.0 %	712.11 551.08 502.92 450.47 322.58 121.0 %	4.09 3.52 3.18 2.92 2.27 80.0 %
3-yr periods (start years: 1980, 1983, 1986, 1989, 1992, 1995, 1998, 2001, 2004, 2007, 2010, 2013, 2016)	Max Q3 Median Q1 Min spread	2.48 2.39 2.30 2.18 2.05 21.0 %	1.62 1.39 1.27 1.25 1.16 40.0 %	669.27 585.00 551.63 531.78 445.09 50.0 %	4.05 3.5 3.30 3.02 2.87 41.0 %
4-yr periods (start years: 1980, 1984, 1988, 1992, 1996, 2000, 2004, 2008, 2012, 2016)	Max Q3 Median Q1 Min spread	2.41 2.38 2.28 2.21 2.11 14.0 %	1.55 1.42 1.30 1.27 1.16 33.0 %	780.34 598.08 549.41 538.84 468.04 67.0 %	3.68 3.51 3.23 2.92 2.87 28.0 %
5-yr periods (start years: 1980, 1985, 1990, 1995, 2000, 2005, 2010, 2015)	Max Q3 Median Q1 Min spread	2.40 2.38 2.27 2.22 2.13 13.0 %	1.43 1.39 1.39 1.25 1.10 29.0 %	785.22 607.16 583.90 554.01 532.12 48.0 %	3.76 3.55 3.30 3.02 3.01 25.0 %
6-yr periods (start years: 1980, 1986, 1992, 1998, 2004, 2010, 2016)	Max Q3 Median Q1 Min spread	2.39 2.32 2.18 2.15 2.13 12.0 %	1.53 1.46 1.41 1.31 1.16 31.0 %	901.35 670.65 651.14 624.83 518.94 74.0 %	3.82 3.68 3.48 3.09 2.90 32.0 %

Table S10: Distribution of capacities for various simulation lengths for the $WECC_g$ $WECC_d$ scenario. This table supports Figure S6. Spread is defined as the relative difference between the max and the min: (max-min)/min x 100.

Simulation length (across 39 years, 1980-2018)	Data type	Total system cost ($/kWh)	Wind cost ($/kWh)	Solar cost ($/kWh)	PGP cost ($/kWh)	Battery cost ($/kWh)
1-yr periods (start years: 1980, 1981, 1982, 1983, 1984, 1985, 1986, 1987, 1988, 1989, 1990, 1991, 1992, 1993, 1994, 1995, 1996, 1997, 1998, 1999, 2000, 2001, 2002, 2003, 2004, 2005, 2006, 2007, 2008, 2009, 2010, 2011, 2012, 2013, 2014, 2015, 2016, 2017, 2018)	Max Q3 Median Q1 Min spread	0.14 0.132 0.129 0.125 0.12 17.0 %	0.055 0.049 0.046 0.046 0.042 30.0 %	0.039 0.032 0.028 0.027 0.019 102.0 %	0.049 0.043 0.038 0.036 0.031 56.0 %	0.018 0.014 0.013 0.012 0.009 90.0 %
2-yr periods (start years: 1980, 1982, 1984, 1986, 1988, 1990, 1992, 1994, 1996, 1998, 2000, 2002, 2004, 2006, 2008, 2010, 2012, 2014, 2016, 2018)	Max Q3 Median Q1 Min spread	0.138 0.134 0.132 0.13 0.127 9.0 %	0.052 0.05 0.047 0.045 0.043 21.0 %	0.036 0.031 0.028 0.027 0.021 76.0 %	0.048 0.046 0.043 0.038 0.036	0.017 0.015 0.013 0.012 0.01 80.0 %
3-yr periods (start years: 1980, 1983, 1986, 1989, 1992, 1995, 1998, 2001, 2004, 2007, 2010, 2013, 2016)	Max Q3 Median Q1 Min spread	0.138 0.134 0.133 0.132 0.127 9.0 %	0.051 0.049 0.047 0.045 0.042 21.0 %	0.036 0.03 0.028 0.027 0.025 40.0 %	0.048 0.045 0.043 0.039 0.037 30.0 %	0.017 0.015 0.014 0.013 0.012 41.0 %
4-yr periods (start years: 1980, 1984, 1988, 1992, 1996, 2000, 2004, 2008, 2012, 2016)	Max Q3 Median Q1 Min spread	0.139 0.136 0.134 0.132 0.13 6.0 %	0.05 0.049 0.047 0.045 0.044 14.0 %	0.034 0.031 0.028 0.028 0.025 33.0 %	0.048 0.045 0.045 0.043 0.041 19.0 %	0.016 0.015 0.014 0.012 0.012 28.0 %
5-yr periods (start years: 1980, 1985, 1990, 1995, 2000, 2005, 2010, 2015)	Max Q3 Median Q1 Min spread	0.139 0.135 0.134 0.133 0.131 6.0 %	0.049 0.049 0.047 0.046 0.044 13.0 %	0.031 0.031 0.03 0.027 0.024 29.0 %	0.048 0.046 0.045 0.044 0.039 25.0 %	0.016 0.015 0.014 0.013 0.013 25.0 %
6-yr periods (start years: 1980, 1986, 1992, 1998, 2004, 2010, 2016)	Max Q3 Median Q1 Min spread	0.139 0.136 0.134 0.133 0.132 5.0 %	0.049 0.048 0.045 0.044 0.044 12.0 %	0.033 0.032 0.031 0.029 0.025 31.0 %	0.048 0.046 0.045 0.042 0.039 21.0 %	0.016 0.016 0.015 0.013 0.012 32.0 %

Table S11: Distribution of cost contributions for various simulation lengths for the $WECC_g$ $WECC_d$ scenario. This table supports Figure S5. Spread is defined as the relative difference between the max and the min: (max-min)/min x 100.

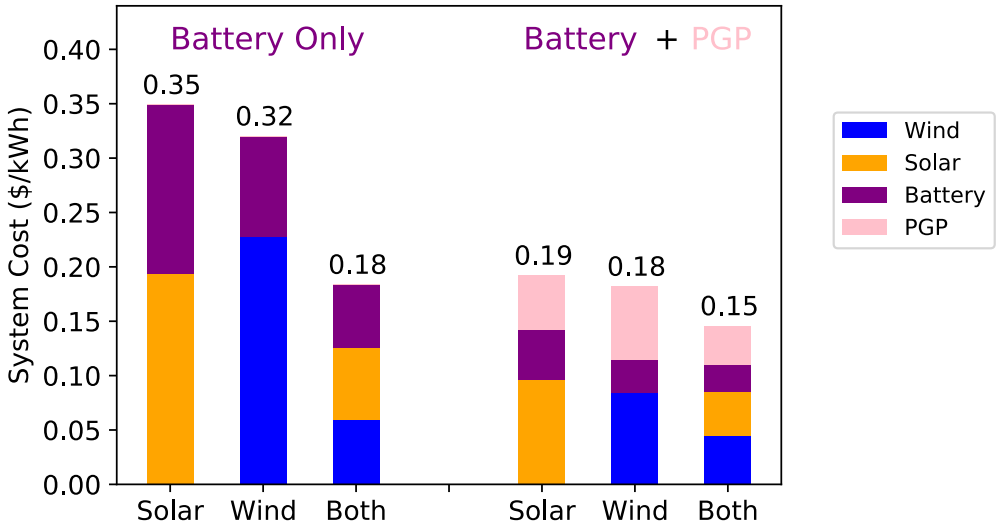

Figure S8: System costs for scenarios meeting California electricity demand with California resources using various generation and storage technologies. The leftmost three bars represent systems with battery storage only and the rightmost three bars represent systems with both battery and PGP storage. Within these groupings, the leftmost bar includes only solar generation, the middle bar includes only wind generation, and the right bar includes both wind and solar generation. Stacked areas in each bar correspond to the total system cost contribution from each technology over the optimization period.

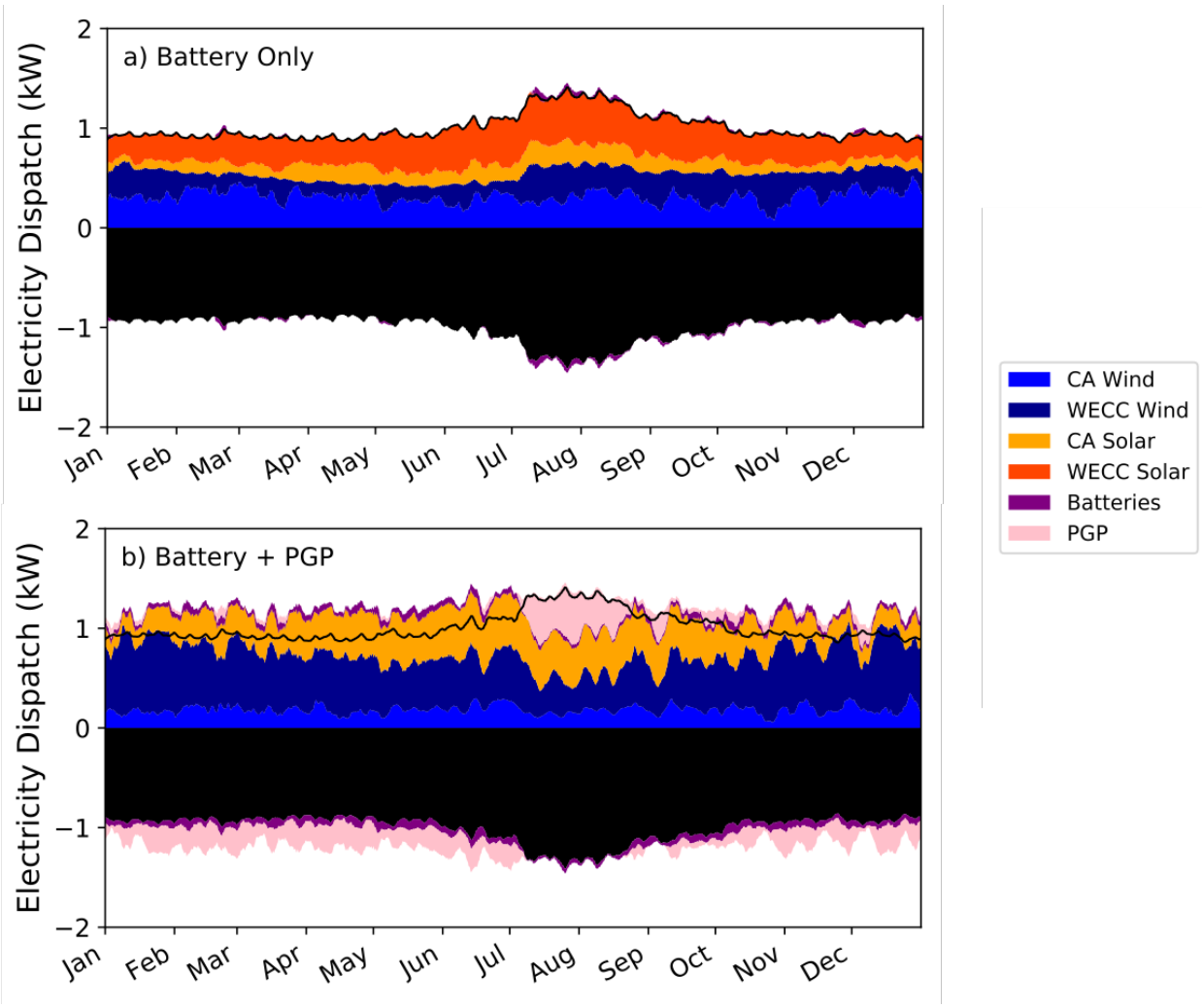

156
157

158 **Figure S9: Dispatch schedule for the WECC$_g$-CA$_d$ cases**. Electricity sources (positive values) and sinks (negative
159 values) to the grid are balanced for each hour during the optimization period (2018). (a) 5-day averaged annual
160 results for a system with battery storage only (b) 5- day averaged annual results for a system with both PGP and
161 battery storage. Generation sources (wind and solar) from both CA and the Western Interconnect and dispatch from
162 storage are balanced by end-use demand and charging of storage for each hour.

163

	Batt only		PGP + Batt	
Wind Capacity (MW)	**Solar Capacity (MW)**	**% Wind of Total Generation Capacity**	**Solar Capacity (MW)**	**% Wind of Total Generation Capacity**
5000	266187	1.84	130987	3.68
10000	254039	3.79	124397	7.44
15000	241891	5.84	117931	11.28
20000	229744	8.01	111640	15.19
25000	218473	10.27	105582	19.15
30000	211568	12.42	98489	23.35
35000	204663	14.60	91800	27.60
40000	197757	16.82	87102	31.47
45000	190852	19.08	81397	35.60
50000	183946	21.37	76048	39.67
55000	177041	23.70	70693	43.76
60000	170136	26.07	66461	47.45
65000	163230	28.48	61031	51.57
70000	155571	31.03	57079	55.08
75000	143690	34.30	-	-
80000	132005	37.73	-	-
85000	120320	41.40	-	-
90000	99268	47.55	-	-

Table S12: Installed solar capacity and % wind of total generation capacity for specified wind capacity optimizations. Results for optimizations where the capacity of installed wind is specified but all other technologies optimize freely. This table supports Figure 5.

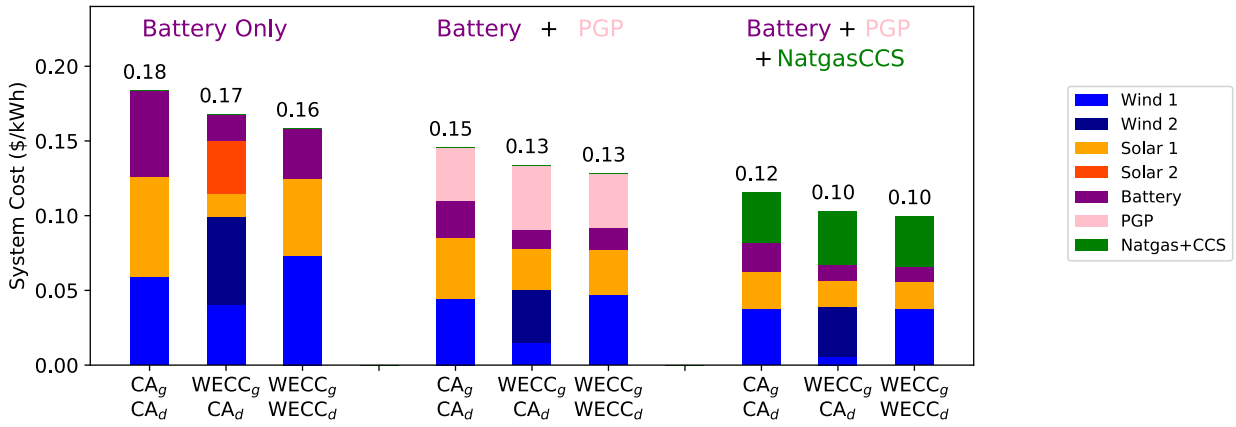

Figure S10: System costs for different resource regions, demand regions, and technology combinations including natural gas with CCS. For bars labeled CA_g CA_d, CA electricity demand is met with CA wind/solar generation. For bars labeled $WECC_g$ CA_d, CA electricity demand is met with wind/solar generation from both CA and the rest of WECC. For bars labeled $WECC_g$ $WECC_d$, WECC electricity demand is met with WECC wind/solar generation. The leftmost three bars represent systems with battery storage only, the middle three bars represent

systems with both battery and PGP storage, and the rightmost three bars represent systems with battery storage, PGP storage, and generation from natural gas with CCS. When included, the annual dispatch of natural gas with CCS was limited to 20% of total demand. Stacked areas in each bar correspond to the total system cost contribution from each technology over the optimization period (2018).

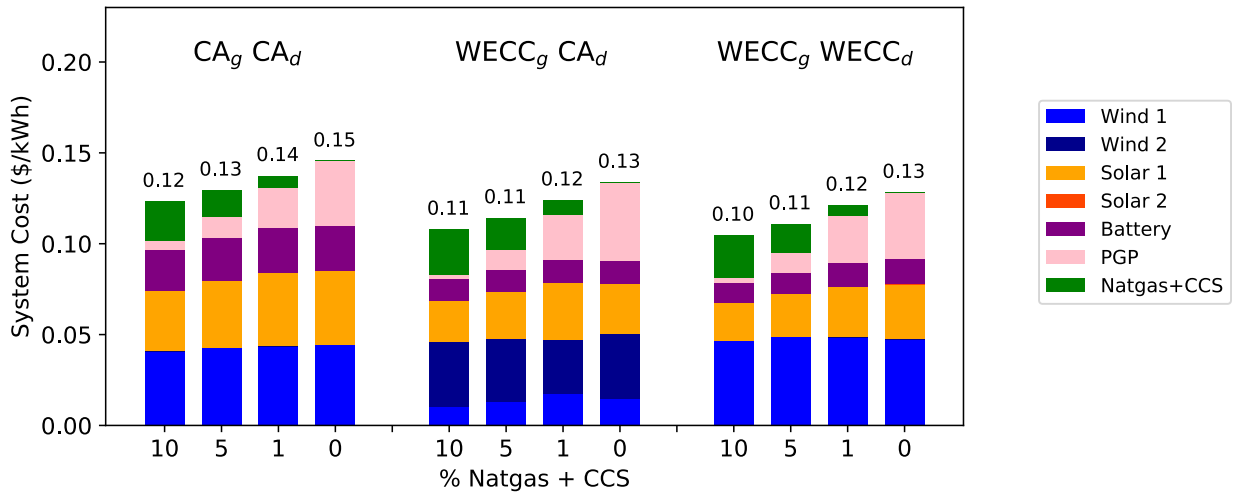

Figure S11: System costs for least cost systems where natural gas + CCS meets 10, 5, 1, and 0% of demand. For bars labeled CA_g CA_d, CA electricity demand is met with CA wind/solar generation. For bars labeled $WECC_g$ CA_d, CA electricity demand is met with wind/solar generation from both CA and the rest of WECC. For bars labeled $WECC_g$ $WECC_d$, WECC electricity demand is met with WECC wind/solar generation. Stacked areas in each bar correspond to the total system cost contribution from each technology over the optimization period (2018). As more natural gas with CCS is allowed in the system, PGP. When annual dispatch of natural gas with CCS is limited to 20% of total demand, PGP is entirely eliminated from the system (Figure S5).

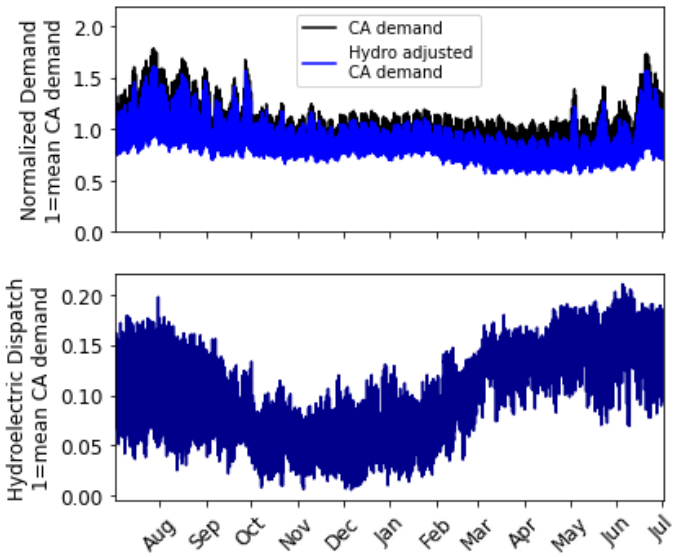

Figure S12: California demand adjusted for hydroelectric dispatch. The top panel shows normalized California demand from July 2016 to July 2017 before (black) and after (blue) subtracting hydroelectric dispatch. The bottom panel shows hourly, historic hydroelectric dispatch from July 2018 to 2019.[1]

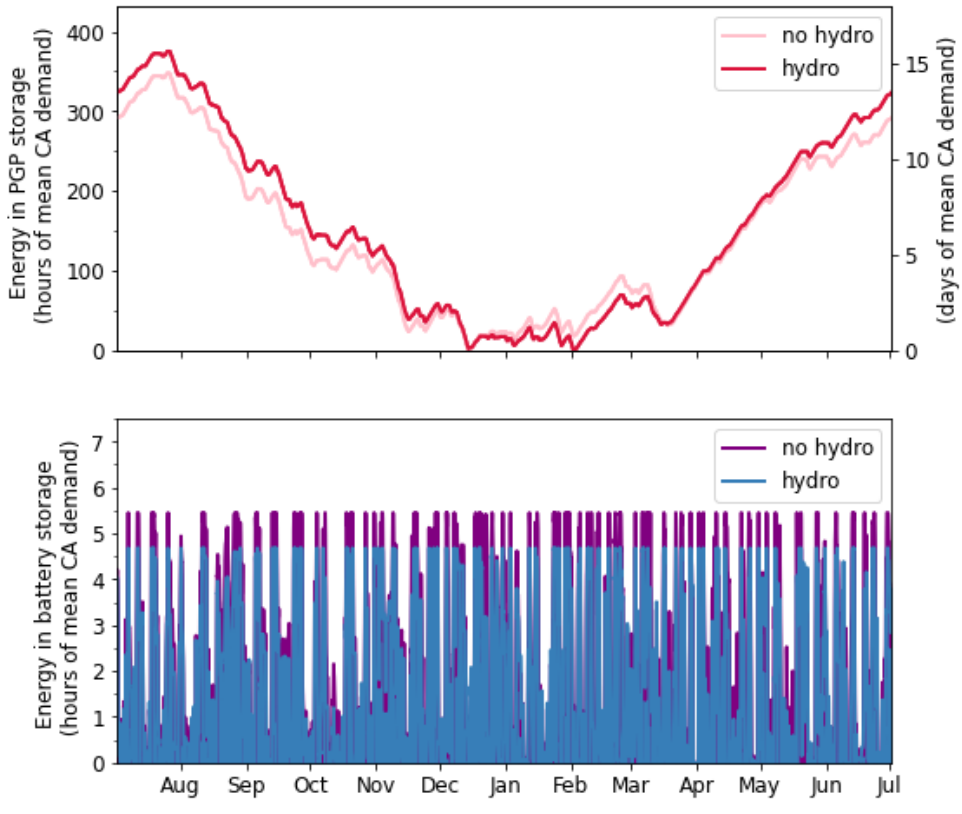

Figure S13: Energy storage during one year for systems with and without hydroelectric dispatch. Energy in PGP storage (top) and battery storage (bottom) over one year from July to July. These results are from optimizations using the normalized CA and hydro adjusted CA demand as described in Figure S6. When hydroelectric dispatch is subtracted from California electricity demand, the resulting least-cost system includes slightly more installed PGP energy capacity (15 days of mean CA demand vs. 14 days without hydro) and slightly less installed battery energy capacity (4.7 hours of mean CA demand vs. 5.5 hours without). The costs of these two systems were fairly similar at 0.14 $/kWh without hydroelectric generation and 0.13 $/kWh with hydroelectric generation.

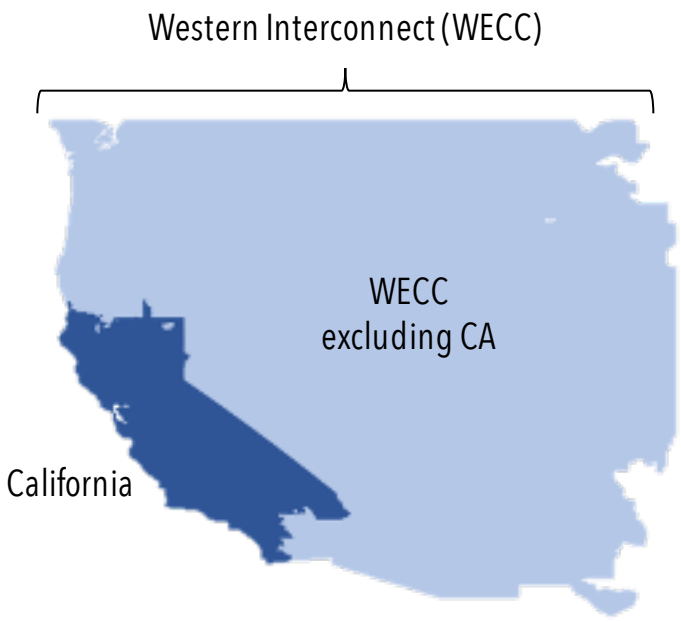

202

203 **Figure S14: Regions used to generate resource datasets**. The plotted shapefiles specify the regions were used to
204 generate the wind and solar resource datasets used in this study. The shapefiles are originally from the
205 Environmental Protection Agency's eGRID Mapping Files.[2] We chose the CAMX region which includes all major
206 cities in California because of its overlap with the balancing authorities (BANC, CISO, LDWP, and TIDC) used in
207 the demand data.

3. *Supplementary cost information*

3.1 Natural gas with carbon capture, sequestration, and storage (CCS)costs

Costs for Natural Gas with CCS	
Technology description	Advanced combined cycle with carbon capture and storage
Total overnight capital cost ($/W)[3]	2175
Fuel cost ($/MMBtu)[4]	3.56[a]
nth-of-a-kind heat rate (Btu/kWh)[3]	7493
Fixed O&M cost ($/kW/yr)[3]	33.75
Variable O&M cost ($/MWh)[3]	7.20
Project life (yrs)[5]	20
Heat content of electricity (Btu/kWh)[6]	3412.14
Calculated levelized costs	
Fixed cost ($/kWh)	0.027
Variable cost ($/kWh)	0.066

Table S13: Cost and technological assumptions for natural gas with CCS. This table supports Figure S9 and Figure S10. For an example calculation of the fixed and variable costs reported in this table, see Section 7.2.
[a]This cost is for natural gas with CCS delivered for electricity generation for the United States. The cost of natural gas with CCS delivered electricity generation for California is slightly higher at 4.5 $/MMBtu, but the US cost was used to maintain consistency in costs isolate the effects of resource availability when comparing different regional examples.

7.2 Example calculation of the fixed and variable costs for natural gas with CCS

These calculations support Table S2.

Efficiency

$$\text{Efficiency} = \frac{\text{heat content of electricity}}{\text{heat rate}} = \frac{3412.14\ \frac{\text{Btu}}{\text{kWh}}}{7493\ \frac{\text{Btu}}{\text{kWh}}\ [39]} = 0.4554$$

Fuel Cost

$$\text{Fuel cost} = \text{fuel cost (thermal)} + \text{fuel cost (electric)}$$

To put everything in terms of $/kWh-electric:

$$\text{Fuel cost} = \frac{\left(\frac{\text{Fuel cost (thermal)}}{\text{heat content of electricity}}\right)}{\text{efficiency}} + \text{fuel cost (electric)}$$

$$\text{Fuel cost} = \frac{\left(\frac{\$3.56}{\text{MMBtu}}\right)\left(\frac{1\ \text{MMBtu}}{0.293\ \text{MWh}}\right)\left(\frac{1\ \text{MWh}}{1000\ \text{kWh}}\right)}{0.4554} + 0\,\frac{\text{mills}}{\text{kWh}} = 0.0267\ \$/\text{kWh}$$

Variable Cost

$$\text{Variable cost} = \frac{\text{Fuel cost}}{\text{Efficiency}} + \text{Variable O\&M costs}$$

$$\text{Variable cost} = \frac{0.0225\ \frac{\$}{\text{kWh}}}{0.4554} + \frac{7.2\ \frac{\$}{\text{MWh}}}{\left(\frac{1000\ \text{kWh}}{\text{MWh}}\right)} = \mathbf{0.0658\ \$/kWh}$$

Capital Recovery Factor

$$\text{Capital recovery factor} = \frac{\text{Discount rate} \times (1 + \text{Discount rate})^{\text{Assumed lifetime}}}{(1 + \text{Discount rate})^{\text{Assumed lifetime}} - 1}$$

$$\text{Capital recovery factor} = \frac{0.07 \times (1 + 0.07)^{20}}{(1 + 0.07)^{20} - 1} = 0.09439 \approx 9.44\%$$

Fixed Cost

$$\text{Fixed cost} = (\text{Capital cost} \times \text{Capital recovery factor}) + \text{Fixed O\&M cost}$$

$$\text{Fixed cost} = \left(\left(\frac{\$2175}{\text{kW}} \times \frac{9.44\%}{\text{year}}\right) + 33.75\frac{\$}{\text{kW} \cdot \text{year}}\right) \times \frac{1\ \text{year}}{8760\ \text{hours}} = \mathbf{0.02727\ \$/kWh}$$

Citations

(1) United States Energy Information. Net generation from hydro for California Independent System Operator (CISO), hourly - UTC Time. https://www.eia.gov/opendata/qb.php?category=3390127&sdid=EBA.CISO-ALL.NG.WAT.H (accessed Sep 22, 2020).

(2) US EPA, O. eGRID Mapping Files: eGRID2016 Subregions https://www.epa.gov/egrid/egrid-mapping-files (accessed Sep 29, 2020).

(3) United States Energy Information (2018). Assumptions to the Annual Energy Outlook 2018: Electricity Market Module. **2018**, 31.

(4) United States Energy Information. EIA Electric Power Annual 2018, Technical report. Table 7.20: Average Cost of Natural Gas Delivered for Electricity Generation by State, 2018 and 2017. https://www.eia.gov/electricity/annual/html/epa_07_20.html?fbclid=IwAR3tnM--aoSr52WrnWQKOQ29rL7G7zoXzZkZH6NfFoLeRudV9vFLvwB9emo (accessed Sep 16, 2020).

(5) United States Energy Information. Assumptions to the Annual Energy Outlook 2018: Commercial Demand Module. Table 2. 2018.

(6) United States Energy Information. Monthly Energy Review – August 2020. Table A6. **2020**, 272.